

**INFLUENCE OF SiC & WALNUT SHELL ASH ON MICROSTRUCTURE  
AND MECHANICAL PROPERTIES OF AA6082 THROUGH FRICTION  
STIR PROCESSING**

A DISSERTATION

SUBMITTED IN PARTIAL FULFILLMENT OF THE REQUIREMENTS FOR  
THE AWARD OF THE DEGREE

OF

MASTER OF TECHNOLOGY

IN

**[PRODUCTION ENGINEERING]**

Submitted by

**[Vikram Saini]**

**(Roll No. 2K21/PRD/17)**

Under the supervision

of

**Prof. VIPIN**

**(Professor)**



**DEPARTMENT OF MECHANICAL ENGINEERING**

**DELHI TECHNOLOGICAL UNIVERSITY**

(Formerly Delhi College of Engineering)

Bawana Road, Delhi-110042

**June, 2023**

## CANDIDATE'S DECLARATION

I, **Vikram Saini**, 2K21/PRD/17 hereby declare that the major project Dissertation titled **“INFLUENCE OF SIC & WALNUT SHELL ASH ON MICROSTRUCTURE AND MECHANICAL PROPERTIES OF AA6082 THROUGH FRICTION STIR PROCESSING”** submitted to the Department of Mechanical, Production & Industrial Engineering, Delhi Technological University, Delhi in fulfillment of the requirement for the award of the **Master of Technology**, in **Production Engineering** was original and not copied from any source without proper citation. This was further to declare that the work embodied in this report has not previously formed the basis for the award of any Degree, Diploma, Fellowship or other similar title or recognition.

Place: Delhi

**Vikram Saini**

Date:

2K21/PRD/17)

## **CERTIFICATE**

I hereby certify that the major project entitled “**INFLUENCE OF SIC & WALNUT SHELL ASH ON MICROSTRUCTURE AND MECHANICAL PROPERTIES OF AA6082 THROUGH FRICTION STIR PROCESSING**”, in partial fulfillment of the requirements for the award of the Degree of Master of Technology in Production Engineering and submitted to the Department of Mechanical, Production and Industrial Engineering of Delhi Technological University has been an authentic record work of **Mr. Vikram Saini (2K21/PRD/17)** carried out under my supervision.

It is to further certify that the matter embodied in this report has not been submitted to any other university or institution by him for the award of any other Degree/Certificate and the declaration made by him is correct to the best of my knowledge and belief.

**Prof. Vipin**

Professor

Department of Mechanical Engineering, Delhi

**Place:** Delhi

**Date:**

## ABSTRACT

Surface modification is a technique used to improve the quality of a surface by making changes to its physical, chemical, or biological properties. In this research, an aluminum AA 6082 Plate is selected, which is been modified by adding small particles of Silicon Carbide and the Walnut shell powder into a groove of 2mm\* 2mm width & depth made on an AA6082 plate. Next, designed an experiment using the Taguchi L9 orthogonal array. After that, based on Taguchi design FSP has been performed on the specimens. Additionally, the specimens were subjected to various tests such as Tensile test, Vickers hardness test, Microstructure test.

In this study, the Taguchi method is carefully analyze and interpret the results obtained from the experiments are: UTS, Yield Stress, and Vickers Hardness. These properties were studied in relation to three key parameters: TRS (RPM), TTS (mm/min), and the weight of walnut shell ash. By examining the effects of these parameters on the mentioned properties, aimed to gain a deeper understanding of their relationship and how they influence each other.

**Keywords:** Friction stir Processing (FSP), Ultimate Tensile Strength (UTS), Tool rotational speed (TRS), Tool Transverse speed (TRS)

## **ACKNOWLEDGMENT**

I would like to express my special thanks of gratitude to **Prof. Vipin** for their guidance, unwavering support and encouragement. This project work could not have attained its present form, both in content and presentation, without his active interest, direction and guidance. His personal care has been the source of great inspiration. He has devoted his invaluable time and took personal care in motivating me whenever I was disheartened.

I would also like to thank Prof. SK Garg, HOD (Mechanical Engineering Department), for their support and guidance, although they had a very busy schedule in managing the corporate and academic affairs.

I am thankful to the Technical staff of Delhi Technological University, Mr. Girish Anand, Mr. OM Prakash, and Mr. Tekchand for their support.

My deep and sincere gratitude to my family for their continuous and unparalleled love, help and support. I am grateful to my brothers for always being there for me as a friend and always with me in every situation. I am forever indebted to my parents for giving me the opportunities and experiences that have made me who I am. They selflessly encouraged me to explore new directions in life and seek my own destiny. This journey would not have been possible if not for them, and I dedicate this milestone to them.

I also want to thank all those who are directly or indirectly support me for my project.

**Vikram Saini**

**(2K21/PRD/17)**

## TABLE OF CONTENTS

<b>CANDIDATE’S DECLARATION</b>	i
<b>CERTIFICATE</b>	ii
<b>ABSTRACT</b>	iii
<b>ACKNOWLEDGMENT</b>	iv
<b>TABLE OF CONTENTS</b>	v
<b>LIST OF TABLES</b>	viii
<b>LIST OF FIGURES</b>	ix
<b>ABBREVIATIONS</b>	x
<b>CHAPTER 1: INTRODUCTION</b>	1
1.1 Friction stir processing	1
1.2 FSP Working principle	1
1.3 Advantage of FSP	1
1.4 Limitations of FSP	2
1.5 Applications of FSP	2
1.5.1 Welding	2
1.5.2 Aerospace industry	2
1.5.3 Automobile industry	2
1.5.4 Surface modification	3
1.5.5 Heat Exchangers	3
1.5.6 Railways	3
1.5.7 Marine industry	3
1.5.8 Additive manufacturing	3
1.6 Effects of tool speed on FSP	3
1.7 Surface modification of AA6082	4
1.8 Methods to prepare AMCs	4
1.10 Properties of silicon carbides	5
1.11 Properties of walnut shell powder	5

<b>CHAPTER 2: LITERATURE REVIEW</b>	6
2.1 Impact on input process variables on surface modification through FSP	15
2.2 Research Gap	16
2.3 Objective of the research study	18
<b>CHAPTER 3: EXPERIMENTAL METHOD</b>	19
3.1 FSP machine setup	20
3.1.1 Tool holder	20
3.1.2 Clamp	20
3.1.3 Force measuring device	20
3.2 Composition and properties of the workpiece	21
3.2.1 Tool material composition and properties	22
3.3 Silicon carbide	24
3.4 Properties of walnut shell powder	25
3.6 Workpiece processing	26
3.7 Sample preparation for tensile test	28
3.8 Sample preparation for micro hardness test	30
3.9 Microstructure testing	34
<b>CHAPTER 4 : METHODOLOGY</b>	34
4.1 Design of experiment	34
4.2 Taguchi method	35
4.3 Minitab software, Signal to noise (S/N) ratio	36
4.4 Design expert software for Regression equation	38
<b>CHAPTER 5: Result and discussion</b>	39
5.1 Orthogonal array	39
5.2 Taguchi analysis	41
5.2.1 UTS : Minitab software, Signal to noise (S/N) ratio	42
5.2.2 UTS : Response table for means	42

5.2.3 UTS: model coefficient S/N ratio	43
5.3.1 Hardness: Minitab software, Signal to noise (S/N) ratio	44
5.3.2 Hardness : Response table for means	45
5.3.3 Hardness: model coefficient S/N ratio	46
5.4 Elongation: Minitab software, Signal to noise (S/N) ratio	48
5.4.1 Elongation: Response table for means	49
5.4.2 Elongation: model coefficient S/N ratio	50
5.5 Results for tensile test	51
5.6 Results for Hardness test	52
5.7 Results for microstructure test	54

## **CHAPTER 6: Conclusion and future scope of study**

6.1 Conclusion	58
6.2 Future Scope of study	59
<b>CHAPTER 7: REFERENCES</b>	60



## LIST OF TABLES

<b>S.No.</b>	<b>Content</b>	<b>Page No.</b>
Table 3.1	FSW machine specification	20
Table 3.2	AA6082 Material composition	21
Table 3.3	Tool material composition	22
Table 3.4	Tool Dimension	23
Table 4.1	Design of experiment	35
Table 4.2	Orthogonal array	36
Table 4.4	Observation table	40

## LIST OF FIGURES

S.No.	Content	Page No.
Figure 3.1	FSP machine used for the Experiment in Advance metal joining lab.	20
Figure 3.2	AA6082 plate	22
Figure 3.3	FSP Tool	23
Figure 3.4	Silicon carbide powder	24
Figure 3.5	Walnut Shell powder	25
Figure 3.6	Grooved AA6082 Plate	26
Figure 3.7	Friction stir processing plates	26
Figure 3.8	Tensile test Specimens	28
Figure 3.9	UTM Machine	29
Figure 3.10	Sample for microstructure and hardness	30
Figure 3.11	Dry polishing.	31
Figure 3.12	Wet Polishing	32
Figure 5.1	Tensile specimens	51
Figure 5.2	Hardness test specimen	52
Figure 5.3	Vickers hardness test	53

## ABBREVIATIONS

ANOVA	Analysis of Variance
CSP	Coconut shell powder
FA	Fly Ash
FSP	Friction Stir Process
FSPed	Friction Stir Processed
FSW	Friction Stir Welding
HYD	Hydraulic
RHA	Rice Husk Ash
SCC	Stress Corrosion Cracking
SEM	Scanning Electron Microscope
SZ	Stir Zone
Temp.	Temperature
TRS	Tool Rotational Speed
TSD	Tool Shoulder Diameter
TTS	Tool Traverse Speed
UTS	Ultimate Tensile Strength
WSP	Walnut shell powder
XRD	X Ray Diffraction
YS	Yield Strength

# CHAPTER - 1

## INTRODUCTION

### 1.1 Friction stir processing

It is one of those process that does not use a filler material or shielding gas. Instead, it uses a tool i.e. non consumable and rotates along the joint line between two metal parts, generating heat and plastic deformation.[1] The tool has a rotating pin with its shoulder having threads, which is dived into workpiece and the tool moves at a controlled speed and force along the joint line. As the tool moves forward, it stirs the metal and creates a plasticized zone, which is then consolidated behind it to form a continuous and defect-free weld.

### 1.2 FSP working principle

The principle of FSP is based on frictional heat generation, which softens the metal and allows plastic deformation to occur. As the rotating tool generates heat and moves along the joint line, the metal becomes soft and malleable. The stirring effect of the tool mixes the plasticized metal and breaks down any oxide layers, resulting in a strong weld with excellent mechanical properties. It can join high-strength materials and produce welds that are free of defects.

### 1.3 Advantages of FSP

In FSP (Friction Stir Processing) there is no need of shielding gas and filler wire. In comparison to conventional welding, there is less distortion. [2] Environment impact factor is less in comparison to conventional welding. The FSP process is carried out quietly. Welding speed of FSP is more than conventional welding.

#### **1.4 Limitations of FSP**

Clamping the workpiece or job in place can be a tedious process when using Friction Stir Processing (FSP) machines. The response time of FSP machines is generally slower compared to other machines, which may affect the efficiency of the process. Additionally, achieving proper intrusion of the tool inside the metal can be challenging as it requires a significant amount of downward force. Despite these challenges, FSP is still a valuable machining process due to its ability to produce high-quality results with minimal material wastage and reduced environmental impact. [3] As with any machining process, it is important to take proper safety measures and follow recommended operating procedures to ensure the best possible outcomes.

#### **1.5 Applications of FSP**

##### **1.5.1 Welding:**

It is used for welding similar and dissimilar metals, such as aluminum, steel, titanium, and copper.

##### **1.5.2 Aerospace Industry:**

It helps in reducing weight, in improving fatigue resistance and corrosion resistance.

##### **1.5.3 Automotive Industry:**

FSP has applications in the automotive industry as FSP leads to production of light weight for joining aluminum alloy which results in increasing fuel-efficiency.

#### **1.5.4 Surface Modification:**

The surface properties of materials can be modified using FSP. It can refine grain structure, improve hardness, and enhance wear resistance and make it suitable for applications such as mining, manufacturing, and tooling.

#### **1.5.5 Heat Exchangers:**

Heat transfer properties of heat exchanger surfaces can be improved on doing FSP by improving microstructures that facilitate efficient heat exchange and improve overall performance.

#### **1.5.6 Railways:**

FSP is used in the railway industry for joining and repairing aluminum and steel components, including train bodies, chassis, and rail tracks. It improves the fatigue resistance and structural integrity of these components.

#### **1.5.7 Marine Industry:**

FSP can be used in the marine industry for joining and repairing aluminum structures that are used in shipbuilding. It provides corrosion resistance, and reduces the risk of galvanic corrosion between dissimilar metals.

#### **1.5.8 Additive Manufacturing:**

Additively manufactured parts can be post processed using FSP to refine the microstructure, to reduce defects.

### **1.6 Effects of Tool speed on FSP**

Both TRS and TTS in welding have an impact on the amount of heat input, which ultimately determines the properties of the welding material and its microstructure. If both rotational & traverse speeds are increased, more heat is generated, resulting in larger grains in the microstructure of the weld. On the other hand, reducing the heat input by decreasing the rotational and traverse speeds leads to smaller grain sizes, which is known as grain

refinement. This is because the lower heat input does not allow the material to fully melt and solidify, resulting in a finer microstructure. On increasing rotational speed of the tool the hardness at the heat affected zone (HAZ) decreases.

### **1.7 Surface Modifications of AA6082**

It is the process of improving surface properties and make it more suitable for the specific application.[4] It can be done physically, chemically or biologically. In today's time modifications of the engineering surfaces is very crucial. Friction stir processing in which heat generated because of the friction causing the material to flow in plastic manner.

### **1.8 Methods to prepare AMCs**

To create Advanced Metal Matrix Composites (AMCs), there are two methods that can be used - Liquid Routes and Solid Route. [5] The Liquid Processing technique is further divided into subcategories. Among these techniques, for the preparation of AMCs the most effective is Friction Stir Processing. This is single step technique for solid processing and is used to achieve micro-structural homogeneity in the material. The process involves using a rotating tool to stir and mix the metal matrix with the reinforcement particles, resulting in a well-distributed composite material.

### **1.9 Reinforcements**

In context of FSP, reinforcements refer to an additional materials or particles that are incorporated into the base material during the process. These reinforcements are intended to enhance specific properties of the material or impart new functionalities.

#### **1.9.1 Particulate Reinforcements:**

Fine particles, such as ceramic or metallic particles, these reinforcements may be added to base material. These particles help in improving mechanical properties like hardness,

strength of material, wear resistance of material. Examples include silicon carbide, alumina, and carbon nanotubes.

### **1.9.2 Fiber Reinforcements:**

Continuous or discontinuous fibers, such as carbon fibers, glass fibers, or metal fibers, can be embedded in the base material. The fibers enhance the material's strength, stiffness, and impact resistance. They are commonly used in metal matrix composites (MMCs) produced through FSP.

### **1.10 Properties of silicon carbides**

Silicon carbide (SiC) is a ceramic material and can be formed in two ways, reaction bonding and sintering. Both forms have wide range of useful properties that are High Strength which make it ideal for applications that requires high strength and stiffness, Hardness which makes it ideal for abrasive applications, and can be used as grinding wheels, cutting tools, High Melting point, Chemical resistance, Thermal Conductivity.

### **1.11 Properties of Walnut shell powder**

Walnut shell powder is a byproduct generated by walnut industry. It has unique physical and chemical characteristics. It is primarily composed of lignin & cellulose. The lignin helps to form a strong bond. The bond enhances the strength of bonding leading to increase in the improvement in the mechanical properties when WSP is used as reinforcement. It also has potential to improve the strength and wear properties



## **CHAPTER - 2**

### **LITERATURE REVIEW**

#### **2.1 Impact of Input process variables on surface modification through FSP**

The literature survey for this project includes a paragraph discussing the selection of the workpiece material, as well as various research studies conducted in the specific area of interest related to the project topic.

Balram Yelamasetti et al. [6] study aimed to enhancement of the surface of AA6061 alloy properties through the incorporation of B4C particles using friction stir processing. The research concluded that dual-pass processing resulted in a more uniform AA6061/B4C surface compared to single-pass processing. In the nugget zone, the average grain size was measured as 8.4  $\mu\text{m}$  for single pass FSP with B4C, and 9.3  $\mu\text{m}$  for dual-pass FSP with B4C. The tensile strength of single-pass processed AA6061/B4C specimens was found to be 11% higher compared to dual-pass specimens with B4C.

Omar S. Salih et al. [7] studied that rotational speed of the FSW tool which has a notable impact on the peak temperature achieved, whereas the transverse speed dictates the duration of exposure and the subsequent rate of cooling. The microstructure of the nugget zone (NZ) displays an elliptical shape and fine equiaxed grains due to the CDR process. Grain growth in the NZ is observed when there is incomplete CDR or prolonged exposure to high temperatures. The welded joint achieved a joint efficiency of 75% compared to the base material (BM), and exhibited a 44% increase in elongation. Among all the tested weld joints, the one welded at a rotational speed of 1500 rpm and traverse speed of 100 mm/min displayed the best tensile properties.

Peng Li et al. [8] The utilization of friction stir processing for the preparation of AlCoCrFeNi<sub>2.1</sub> HEA particle reinforced aluminum matrix composites yielded composites without any defects. These composites exhibited uniform distribution of particles and sound bonding at the interface. After undergoing six passes of friction stir processing (FSP), The

incorporation of HEA reinforcement in the composite played a crucial role in grain refinement and particle enhancement. As a result, the composite exhibited an increase in hardness and tensile strength by 28.6% and 25.6% respectively, compared to the FSPed-6061 material. The tensile strength of the FSPed-6061 sample improved to 306.8 MPa, while the 15%-AMCs sample exhibited a higher tensile strength of 332.1 MPa. After undergoing heat treatment, the age-reinforcement phase precipitated in the aluminum alloy matrix. This resulted in a significant increase in strength for both samples, with a 72.8% increase for the FSPed-6061 sample and a 49.0% increase for the 15%-AMCs sample, compared to their respective strengths before heat treatment.

N. Yuvaraj et al. [9] used a combination of fusion and solid-state processing techniques to create aluminum composites by adding Boron carbide into Aluminum 5083. Two methods were employed: The Tungsten Inert Gas (TIG) arc process and Friction Stir Processing (FSP). The researchers performed experiments on chosen specimens, applying a rotational speed (TRS) of 1070 rpm, traverse speed (TTS) of 40mm/min, and a plunger force of 40 KN. The results showed that the composites created through FSP had a greater thickness compared to those made using the TIG method. The TIG-based specimens showed greater hardness and resistance to wear compared to the TIG arc-based specimens. However, the TIG-based specimens had lower micro hardness than the TIG arc-based specimens. On the other hand, the wear resistance of the TIG-based specimens was lower than that of the FSPed specimens.

Sharifitabar et al. [10] the main objective of the researchers is to analyzed the mechanical properties and microstructure of these composites. They discovered that increasing the number of passes in FSP resulted in a more even distribution of nanoparticles within the composite material. This improved distribution allowed for better control over the material's properties. Furthermore, with an increase in the number of passes, the size of the grains became smaller, resulting in a notable increase in both tensile and yield strength. Additionally, the material exhibited improved elongation, indicating enhanced flexibility and ductility.

Moslem Paidar et al. [11] The researchers investigated how B4C particles fragmented and dispersed within the aluminum matrix when using multiple FSP passes. They observed that as the number of FSP passes increased, the fragmentation and dispersion of B4C particles improved.

As the number of passes increased, the grain size decreased significantly, indicating grain refinement within the material. As the number of FSP passes increased from 1 to 8, the tensile strength of the composite also increased. The strength values showed a significant improvement, ranging from 86.84 MPa to 173.92 MPa. Moreover, with the increase in FSP passes, the composite exhibited reduced wear losses and a lower wear rate, ranging from  $6.198 \times 10^{-5}$  to  $1.095 \times 10^{-5}$  mm<sup>3</sup>/Nm. additionally, the friction coefficient decreased, with the upper boundaries and there was a decrease in the friction coefficient from 0.56 to 0.19.

P K Mandal [12] The study found that the friction stir process (FSP) effectively modifies the surface of aluminum alloys, improving their ductility by eliminating porosity and breaking up coarse second phase particles. The Multi Pass-FSP alloy showed remarkable improvement in its tensile properties. It had a 251.5 % increase in 0.2 % proof strength, a 122.48% increase in ultimate tensile strength, and a high ductility of 42.55%. However, it had a lower hardness of 4.84% compared to the Double Pass-FSP alloy. Optical micrographs showed that the FSP process with low heat input resulted in fine grain size for alloy 1 ranged from 2 to 6 micrometer while for Alloy 2, it ranged from 4 to 8 micrometer.

Essam B. Moustafa et al [13] The study examined the use of Friction Stir Processing (FSP) in two distinct alloys: AA5052 and modified AA5050 with added TiB. The size of grains in the original 5052 alloy was reduced to approximately 8 mm after the second pass. On the

other hand, the modified 5052 alloy containing TiB exhibited grain refinement of around 12.5  $\mu\text{m}$ . It was observed that the TiB additives hindered grain refinement during FSP.

Seyed Sajad Mirjavadi et al [14] After conducting an investigation, it has been observed that carrying out multiple iterations of friction stir processing (FSP) on AA5083 sheets, specifically using Two, Four, Six, and Eight passes, consistently enhances their strength and hardness.

This is achieved by continuously refining the microstructure and evenly distributing reinforcement particles, as observed in the microstructure.

Sumit Choudhary, et al [15] Defect-free friction stir welded (FSW) joints of the AA5086-H116 alloy, significant accomplishments were attained, exhibiting a joint efficiency of approximately 94% were achieved. This efficiency was further improved to approximately 95% and 98% in joints reinforced with copper (Cu) When subjected to an iteration (Single pass Copper) and two successive passes (Double pass Copper) during processing, the material demonstrated notable alterations. The microhardness of the joints also showed improvement, with an increase of approximately 15% and 13% in the Single pass copper and Double pass copper joints respectively.

The fatigue and endurance thresholds of both the Single pass copper and Double pass copper joints exhibited similar results, with a collective improvement of approximately 18% compared to standard weld joints (W).

Essam B. Moustafa et al [16] In this study, A nanocomposite with a hybrid composition consisting of AA7075/Boron nitride NbC, AA7075/Boron nitride SiC, and AA7075/Boron nitride TaC was created using the method of friction stir. The fabrication process involved the solid-state processing was conducted at 85% of the melting temperature of the base alloy AA7075, which proved to be successful in achieving optimal heating conditions. As a result, the average grain size decreased by an impressive 2880%, from a base size of 17928  $\mu\text{m}$  to just 4.61.2  $\mu\text{m}$  in the composite.

M. Saravana Kumar et al [17] An examination was conducted on hybrid metal matrix composites, comprising and 5% of B<sub>4</sub>C reinforcement particles with 5% of fly ash which exhibited minimal particle clumping and clustering at the grain boundaries. The composite that displayed optimal characteristics consisted of an optimal combination 5% of boron carbide and of 5% of fly ash. The maximum tensile strength achieved was 184.72 N/mm<sup>2</sup>, signifying the highest value observed. This value was 3.4% higher than composites with 10% flyash reinforcement and The tensile strength of the composite was 18.7 percent greater compared to the unreinforced Al\_Mg\_Si-T6 alloy, representing a substantial improvement. However, its hardness value decreased when the fly ash content reached 20% due to particle agglomeration and clustering.

Safiye Ipek Ayvaz et al. [18] SiC reinforced surface composites were made successfully in one attempt, but there were issues with clustering in B<sub>4</sub>C reinforced surface composites, the sizes of the grains were measured as 5.38 μm for the non-reinforced sample, 4.32 μm for B<sub>4</sub>C reinforced surface composites, and 2.66 μm for SiC reinforced surface composites. After the process of friction stir, the value of hardness of all surface composites increased, including B<sub>4</sub>C and SiC reinforced ones, as well as the non-reinforced surface composites. Among the samples, the SiC-reinforced one exhibited the highest hardness, measuring 89.7 HV, while the B<sub>4</sub>C reinforced sample has a maximum hardness of 88.1 HV.

Mohd Rashid et al. [19] studied that on doing FSW joint using Nani-TiC reinforcement in AA6082-T651 alloy, the micro hardness found to be higher by small quantity in comparison to parent metal and the strength of the welded joints is partially restored by the inclusion of TiC.

B. Praveen KUMAR et al. [20] et al. When examined the composite material consisting of an aluminum metal matrix and Ash of bamboo leaf by stir casting, it was found that SiO<sub>2</sub> (silicon dioxide) was a major component. As the content of BLA increased in the composite, the density of the fabricated composites decreased compared to the Al 4.5% Cu alloy. The

composite exhibited a maximum porosity of 2.512%, which corresponded to a 6% content of BLA. As the content of BLA increased relative to the matrix, the hardness of the composites demonstrated a corresponding rise. The strength of the composites, both in terms of tensile and yield, showed improvement as the amount of BLA increased by 2 percent, 4 percent, and 6 percent in comparison to the matrix. The highest values for both tensile and yield strengths were observed when the composite contained 4 percent BLA particles. However, it is worth noting that the ductility of the composite, as indicated by its elongation, decreased in comparison to the matrix.

Rajeev Kumar et al. [21] The sample made at 1600 rpm exhibits a higher coefficient of friction (COF). The Fast Fourier Transform (FFT) analysis regarding the vibration signal indicates, during the processing at various RPM & feed rates, the graphs follow a similar pattern. When the feed rate was set at 30 mm/min, the analysis of vibration signals indicated that at 1600 rpm, there was less unpredictability observed. This observation suggests that the optimal parameters for achieving successful friction stir processing of AA7075 combined with B4C particles are a feed rate of 30 mm/min and a rotational speed of 1600 rpm. The base material wears out more quickly compared to the MMC (Metal Matrix Composite) samples. Among all the samples tested, the one made with hard B4C particles at 1600 rpm shows the least amount of wear

Nitesh Kumar et al. [22] The FESEM images show that both SiC and secondary reinforcement materials Powder of chicken bone, powder of walnut shell, Powder of rice husk are spread out evenly within the area where the matrix material is being stirred. The average size of the grains in the created specimens falls within the range of 20 to 35 micrometer for all three types of composites. The smallest size of the grain notices 6 micrometer in the Al6082 and 2 percent SiC and 2 percent walnut shell powder composite. The study of EDS spectrum and phase mapping shows that The reinforcing phase is thoroughly mixed or integrated into the matrix material. AN increase of 20 to 35 percent of tensile strength has been observed in samples in comparison to the base alloy

Alaneme et al. [23] studied that as the weight percentage increases then the value of tensile strength and hardness also increases. However, the value of hardness and strength value decreased when the content of GSA (groundnut shell ash) increased. The decrease in the value of strength and hardness observed when composites containing GSA was less than what was seen in composites reinforced with RHA (rice husk ash) and BLA (bagasse ash), with increase in ground nut shell powder the elongation is improved slightly. But there was no consistent trend observed on increasing the ratios of silicon carbide and groundnut shell ash by weight. The fracture toughness improved as the content of ground nut shell ash increase. Groundnut shell ash can be effectively used as a reinforcing material to produce low-cost, high-performance aluminum matrix composites. Even at higher weight fractions, Groundnut shell ash has a positive impact on mechanical properties in comparison to RHA and BLA.

N. Li et al. [24] In this study a CoCrFeNiCu alloy having 320 nanometer of grain size, was created using friction stir processing. Initially the microstructure of the alloy remains stable even during heat treatment. The friction stir processed CoCrFeNiCu alloy showed exceptional superplasticity, with elongation of over 600% when the process was carried out at a temperature of 950°C and the value of strain rate is  $3 \times 10^{-3} \text{ s}^{-1}$ . This high superplasticity is mainly attributed to the balanced distribution of high angle grain boundaries. Additionally material showed thermal stability.

T M Harish et al. [25] studied that on adding CCSA (Crushed Coconut Shell Ash) to Al5083, we can enhance the alloy's properties and contribute to environmental sustainability by utilizing waste material. FSP leads to the breaking down of particles, redistribution of the second phase, refining of the grains, and a partial interaction between the coconut shell ash and Aluminium. This interaction results in the formation of an Al<sub>4</sub>C<sub>3</sub> compound. Results shows an increase in the hardness of the surface composites when crushed coconut shell ash and boron carbide are used. Among the hybrid composites, the Al5083-5% B<sub>4</sub>C and 3

percent Coconut Shell Ash composite has the highest value of tensile strength that is 239.62 MPa, while the tensile strength of value 125 MPa was observed when 5 percent Boron carbide and 8 percent of Coconut Shell Ash composite is used. As the amount of reinforcement material increases, the agglomeration of the particles leads to a gradual decrease in the ultimate tensile strength.

Gaurav Rajan et al. [26] Applied FSP on the nanocomposites led to the creation of small recrystallized grains and the SiC particles were also evenly distributed. This was confirmed through microscopy techniques. The FSP also eliminated casting defects and improved the overall structure. The material contains additional precipitates rich in manganese. The yield strength of the Friction stir processed samples were significantly improved compared to their cast counterparts. However, the 3 percent of composite showed a deterioration in mechanical properties such as tensile due to premature failure caused by clustered nanoparticle regions.

Xiguo Chen et al [27] the study examined a composite material made of the nanoparticles of titanium oxide & tricalcium phosphate. Phase analysis showed that the sample composed of nanoparticles demonstrated did not undergo any changes in phases and the temperature variations. This is because the temperature did not reach a point where the melting of nanoparticles of titanium oxide & tricalcium phosphate does not take place. Weight analysis in a PBS solution (phosphate-buffered saline) revealed that the analysis indicated that samples containing a larger quantity of titanium oxide compound exhibited reduced weight loss, primarily due to chemical bonding.

Yuchen Peng et al [28] studied that on using HRS-SFSP (High rotating speed submerged friction stir processing) at a speed of 3600 rotation per min, the grain in the processed zone became finer with size of 3.21 micrometer and the material possessed a high proportion of grain boundaries. However, as the rotating speed was raised to 5400 rotation per min, the



grain started to become larger, resulting in the decrease in corrosion resistance.

Ibrahim H. Zainelabdeen et al [29] the use of FSSur.P (friction stir surface processing) resulted in significant grain refinement and a more even distribution of grains. However, increasing the rotational speed led to a slight increase in grain size. The Friction stir processed samples showed an increase in the value of micro hardness. Additionally, a clear improvement in the elastic modulus was observed in all processed samples. The samples that underwent processing showed a substantial enhancement in their ability to resist corrosion when compared to the original or base metal. Furthermore, there was a strong agreement between different electrochemical methods used to measure corrosion.

Changshu He et al [30] The microstructure of the wire-arc additive manufacturing (WAAM) 4043 aluminum alloy consists of alpha Aluminium dendrites and a network of Silicon rich eutectic phase. Manufacturing defects in the form of gas pores are also present. After applying the interlayer FSP (friction stir processing) deformation the majority of the pores are eliminated, and the alpha Aluminium dendrites (crystalline structures) and Siliconrich eutectic network (composition) are fragmented or disrupted. The WAAM (Wire Arc Additive Manufacturing) + interlayer FSP (Friction Stir Processing) components possess a yield strength (YS) of 88 MPa and an ultimate tensile strength (UTS) of 148 MPa. And the Elongation is improved by at least 108.7%. This improvement can be attributed to two factors: the fragmentation of the Silicon-rich eutectic phase and the reduction in grain size resulting from the deformation caused by interlayer FSP.

Suhong Zhang et al [31] found that Friction stir processing (FSP) is an effective method to create bulk composites using AA7075 with 10 weight% of Ni nanoparticles. The composites are strengthened by the formation of in-situ Al<sub>3</sub>Ni nanoparticles. XRD phase analysis shows that FSP transforms 93% of the Ni into the Al<sub>3</sub>Ni phase in the composite. AA7075 after performing FSP have Vickers hardness values of 92.1 HV and 126.7 HV in the initial processed state, both with and without the addition of Nickel (Ni), After T6 aging, its value of hardness increases.

S. Ragu Nathan et al. [32] surface composites are created by adding reduced graphene oxide (RGO) particles using the friction stir process. The RGO 5 Pass specimen showed an improved thermal conductivity of 38% compared to the base matrix. This is because the frictional heat and plasticization process reduce the oxygen content in RGO, increasing its conductivity. However, the FSPed specimens have lower thermal conductivity than the base matrix the hindered transfer of heat is attributed to the increased number of grain boundaries, impeding the heat flow. The formation of a mechanically mixed layer containing Al<sub>2</sub>O<sub>3</sub> and Fe<sub>2</sub>O<sub>3</sub> in the five Pass specimen reduces the rate of wear.

A.K. Basak et al. [33] studied Friction Stir Processing (FSP) on Al 5086 fabricated with SiC and Gr reinforcements based surface composite. The surface composites showed higher yield strength compared to the bulk Al-alloy. The yield strength for the 5/15 and 5/30 composites was 127.9 MPa and 151.2 MPa, respectively, whereas the bulk Al-alloy had a yield strength of 93.5 MPa. Similarly, the ultimate compressive strength of the surface composites (155.4 MPa and 1693.3 MPa) was also higher compared to the bulk Al-alloy (147.8 MPa). In the bulk alloy, deformation was mainly characterized by strain bursts. However, in the surface composite, the reinforcing particles played a dominant role in the deformation mechanism. The initial loading was accommodated by the formation of slip/shear bands, followed by load transfer between the reinforcements and the matrix.

Wenchang Li et al. [34] studied on adding carbon fiber to the material. Effectively. It has been found that composite joint attained its maximum hardness when carbon fiber was introduced at a depth of 1 mm and when the welding speed was set at 20 mm/min. Compared to the starting material H62 brass matrix without CF, the composite that was created through Friction stir processing with carbon fibre showed an increase in hardness ranging from 14.1% to 29.8% and 36.1% to 54.9%. The wear of the composite material prepared with Carbon fibre through stir friction processing was significantly lower (around 15.5%-41.0%)

when compared to H62 brass matrix without carbon fibre.

Krunal M. Mehta et al. [35] Surface composites using B<sub>4</sub>C created using friction stir processing (FSP) have significantly improved in the wear resistance in comparison to base metal. Wear of composites is reduced by about 74-87% compared to base metal. The way the powder is applied significantly impacts the wear characteristics of the composites, with the Hole method proving to be superior to the Slot method. The superiority of the Hole method is attributed to the finer refinement of the reinforcement particles in the composite. The hole method resulted in more uniform distribution of reinforcement particles within the matrix, leading to improved overall performance. homogeneous processed zone. This uniform distribution of harder B<sub>4</sub>C particles leads to higher hardness and improved wear resistance.

## **2.2 Research Gap**

The research gap in the development of Friction Stir Processing (FSP) using reinforcement of silicon carbide (SiC) are:

### **2.2.1 Optimization of Reinforcement Dispersion**

Is needed to optimize the dispersion of SiC particles within the matrix material during FSP. Achieving a uniform and controlled distribution of SiC reinforcements throughout the material is crucial to maximize their strengthening effects and ensure consistent properties in the resulting composite.

### **2.2.2 Characterization of Composite Properties:**

Comprehensive characterization of the mechanical, thermal, and tribological properties of SiC-reinforced FSP composites is necessary. This includes evaluating properties such as hardness, strength, fracture toughness, wear resistance, and thermal conductivity. Understanding the relationship between FSP parameters, reinforcement content, and resulting

properties will facilitate the design and optimization of SiC-reinforced FSP materials for specific applications.

### **2.2.3 Microstructural Analysis:**

Detailed microstructural analysis, including examination of grain structure, interfacial bonding, and particle distribution, is needed to gain insights into the reinforcement mechanisms and identify any microstructural defects or inconsistencies that may affect the composite's performance.

### **2.2.4 Long-Term Performance and Durability:**

Investigating the long-term performance and durability of SiC-reinforced FSP composites is crucial for assessing their suitability for practical applications. This includes evaluating factors such as fatigue resistance, creep behavior, corrosion resistance, and resistance to environmental degradation over extended service life.

### **2.3 Objective of the Research Study**

On the basis of an extensive research survey, the following research objectives have been derived.

1. In order to improve the mechanical characteristics of an AA6082 plate, one can enhance the surface of the metal through a process known as Friction Stir Processing (FSP).
2. To create specimens of AA6082 measuring 200mm×80mm×6 mm, the following dimensions are utilized.
3. To create a hybrid reinforcement for the deposition of SiC and walnut shell powder ash as reinforcement layers.
4. To find out the impacts of factors, including Rotational Speed of tool in (RPM), Transverse Speed of tool in (mm/min) and weight of walnut shell powder ash and SiC, the following parameters are considered for analysis.
5. The microstructural analysis is conducted on the samples using an optical microscope to examine their micro structure.
6. To investigate the influence on Tensile strength, Yield Strength, percentage elongation and Vickers Hardness, the effects are carefully examined and analyzed.

## **CHAPTER- 3**

### **EXPERIMENTAL SETUP**

#### **3.1 FSP Machine Setup**

Friction Stir processing machine can be used on AA6082 series. The complete specifications of the machine are given in the table. FSP machine has 3 phase motor.

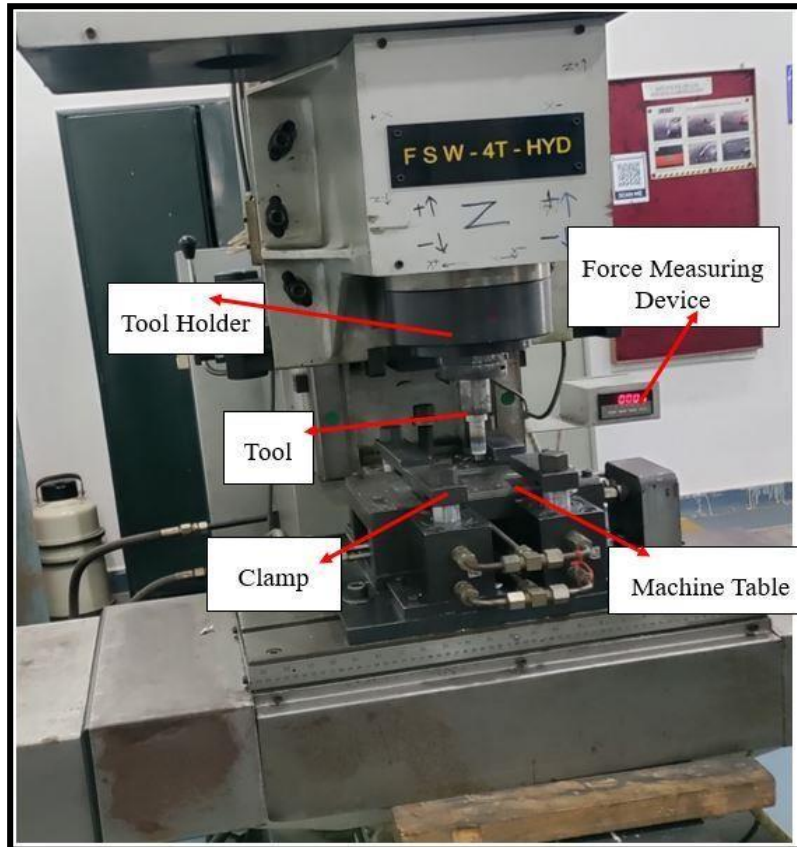
Friction Stir processing machine can be used on AA6082 series. The complete specifications of the machine are given in the table. It has 3 phase motor which helps in rotation and translation motion of the tool. It has hydraulic system for the clamping of the work piece, Up & Down movement of the tool and the base translation movement. With help of knob for actuators the hydraulic system is discharged.

**3.1.1 Tool Holder:** The tool holder securely holds and positions the FSW tool during the processing process.

**3.1.2 Clamp:** The clamp holds the workpieces firmly in place, maintaining proper alignment and preventing any movement or misalignment during the processing.

**3.1.3 Force Measuring Device:** The force measuring device monitors and measures the applied forces during the processing. It provides real-time feedback on the forces exerted by the FSP tool, allowing for process control and optimization.

During this experiment, Friction Stir Processing (FSP) was conducted on various parameters including Tool Rotational Speed (RPM), Tool Translational Speed (mm/min), and the hybrid reinforcement comprising SiC and walnut shell powder.



<b>Machine Specification</b>	
Machine Size(L*B*H)	1300x1650×2000 mm
Table Working Surface	600×400 mm
Machine Total weight	2 Ton
Welding Materials	MS, Al, Cu
Job Size Maximum (Thickness)	5 mm
Welding Geometry	Straight
<b>Machine travel</b>	
x-axis	600 mm
y-axis	200 mm
z-axis	300 mm
<b>Axis thrust force</b>	
x-axis	250-2500 Kgf
y-axis	400-4000 Kgf
<b>Motion</b>	
x-axis travel speed	0-5000 mm/min
y-axis travel speed	0-2000 mm/min
<b>Spindle housing</b>	
spindle	ISO 40 taper
spindle speed	1440 RPM (max)

Table 3.1 FSW machine specification

### 3.2 Composition and properties of the workpiece

For the experiments conducted, AA6082 was selected as the material for the workpiece

<b>Chemical Composition</b>	<b>Percentage Present</b>
<b>Iron</b>	<b>0.0 - 0.50</b>
<b>Manganese</b>	<b>0.40 - 1.00</b>
<b>Magnesium</b>	<b>0.60 - 1.20</b>
<b>Silicon</b>	<b>0.70 - 1.30</b>
<b>Copper</b>	<b>0.0 - 0.10</b>
<b>Zinc</b>	<b>0.0 - 0.20</b>
<b>Titanium</b>	<b>0.0 - 0.10</b>
<b>Chromium</b>	<b>0.0 - 0.25</b>
<b>Aluminium</b>	<b>Balance</b>

*Table3.2 AA6082 Material Composition*



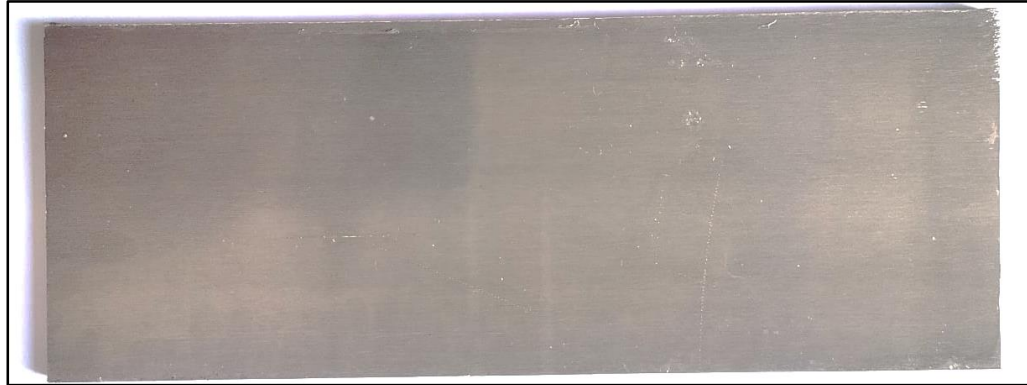


Figure 3.2 AA6082 Plate

### 3.3 Tool Material Composition and Properties

As carbon content in the tool increase the hardness of the material increases but loses its ductility. Mild steel possesses certain physical properties such as High Tensile strength, High impact strength and good ductility. This means that it is capable of withstanding high levels of tension, can absorb heavy impacts without breaking, Mild steel rod of diameter 32mm has been taken from machining workshop and then it was machined on lathe machine to form the FSP Tool with specific dimensions.

Table 3.3 Tool Material composition

Iron	C%	Si %	Mn %	S %	P %	Fe %	Cu %
Mild steel	0.29	0.28	0.10	0.10	0.04	98.14	0.20

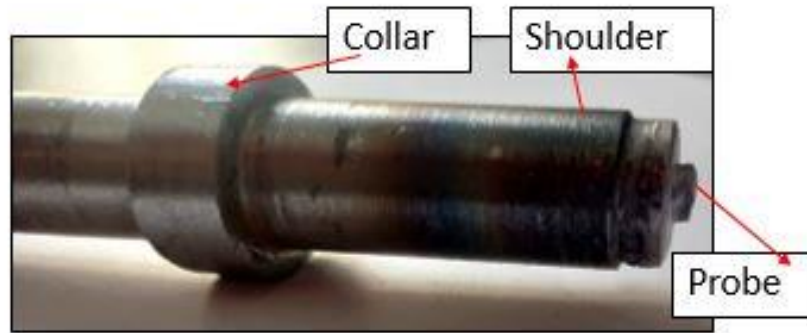


Figure 3.3 Friction stir processing tool

Table 3.4 Tool Dimension

<b>Collar Diameter</b>	<b>28mm</b>
<b>Shoulder Diameter</b>	10mm
<b>Collar thickness</b>	19.8mm
<b>Probe Thickness</b>	3mm
<b>Probe Diameter</b>	6mm

### **3.3 Silicon Carbide (SiC)**

Silicon carbide is a versatile material known for its exceptional properties. It possesses characteristics including high hardness, exceptional thermal conductivity, and exceptional resistance to wear, corrosion, and extreme temperatures. These characteristics make it suitable for various applications, including cutting tools, abrasives, refractories, and semiconductors.



*Figure 3.4 Silicon carbide powder*

### **3.5 Properties of Walnut Shell Powder**

Walnut shell powder is a byproduct generated by walnut industries. It possesses distinct physical and chemical properties that are unique to its composition. It is primarily composed of cellulose and lignin. The incorporation of walnut shell powder as reinforcement leads to enhanced mechanical properties. It has the potential to improve both strength and wear characteristics of the material.



*Figure 3.5 Walnut shell powder*

### **3.6 Workpiece processing**

In the experiment, the procedures were carried out as per the pre-determined design of the experiment. The tilt angle was established at  $1^\circ$ , taking into account previous research findings. conducted a series of nine experiments on the grooves of AA 6082 plates, following a design matrix that incorporated different Tool Rotational Speeds (TRS), Tool Translational Speeds (TTS), and varying sample sizes, as illustrated in Figure (3.6). The experimentation was conducted using the FSP machine.

A groove with a depth and width of 2mm was meticulously created on each of the 9 aluminum plates. This was done to facilitate the infusion of the hybrid reinforcement consisting of SiC and walnut shell powder.

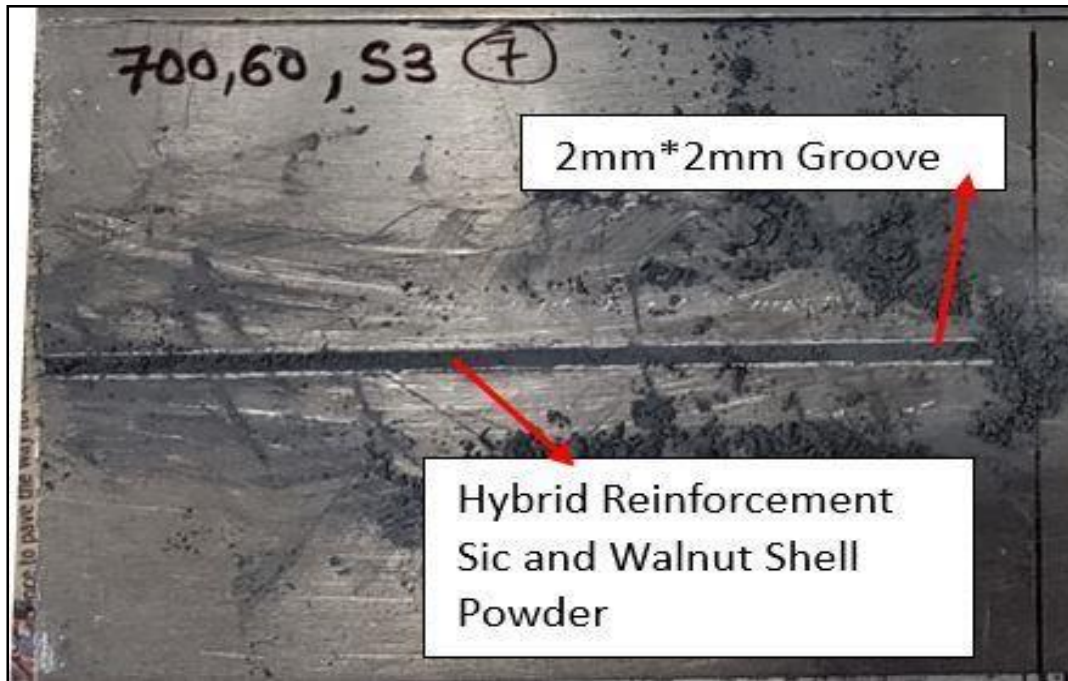
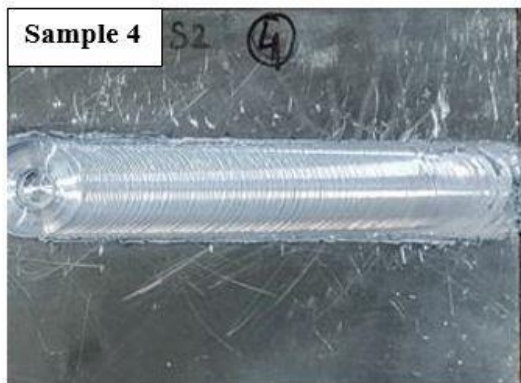
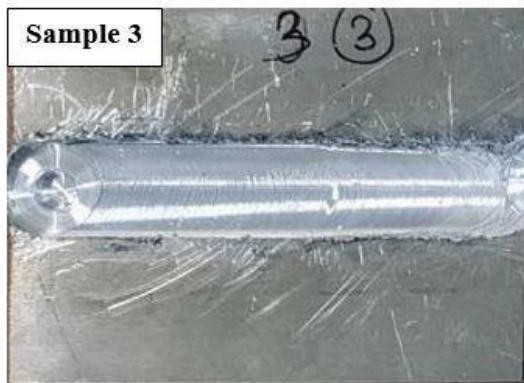
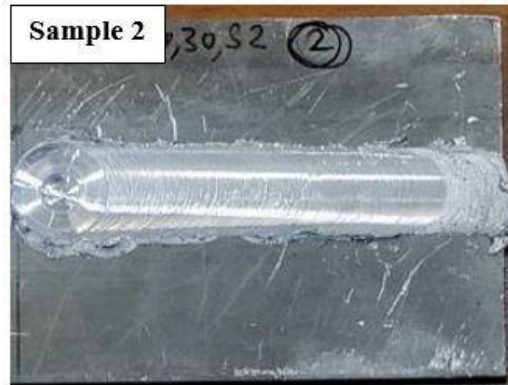
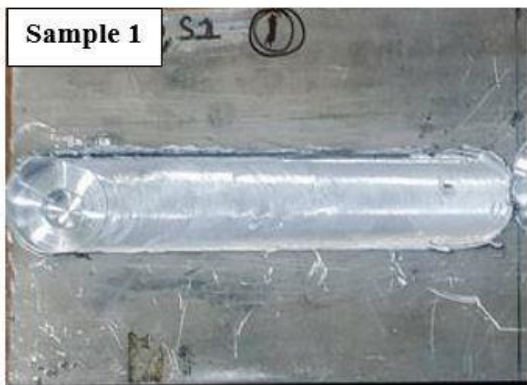
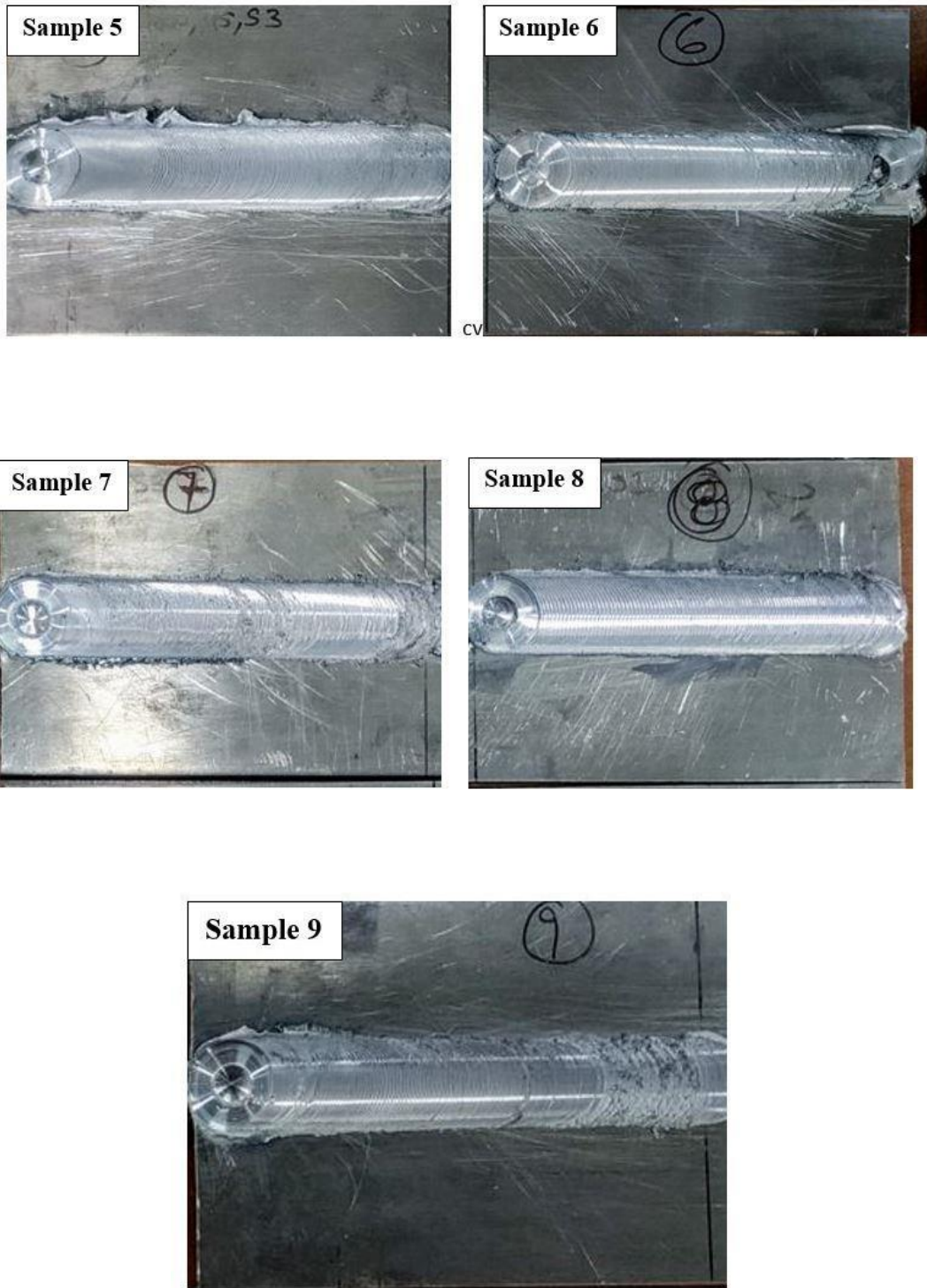


Figure 3.6 Grooved AA6082 plate



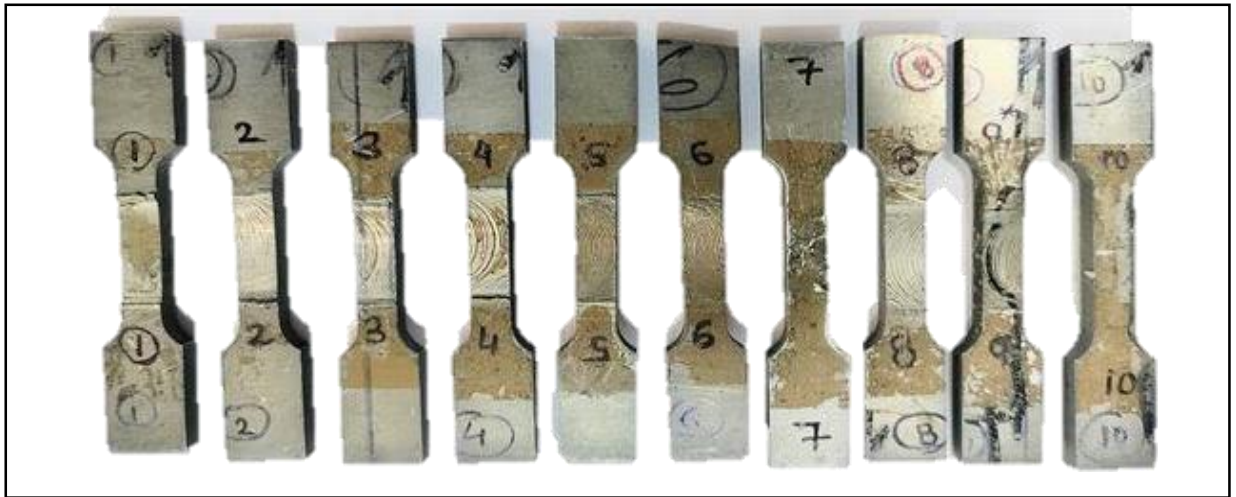


*Figure 3.7 Friction stir processed plates*

### 3.7 Sample Preparation for Tensile Testing

The samples were prepared specifically for conducting tensile testing.

Tensile specimens were fabricated by utilizing wire electro discharge machine at the workshop.



*Figure 3.8 Tensile test specimens*

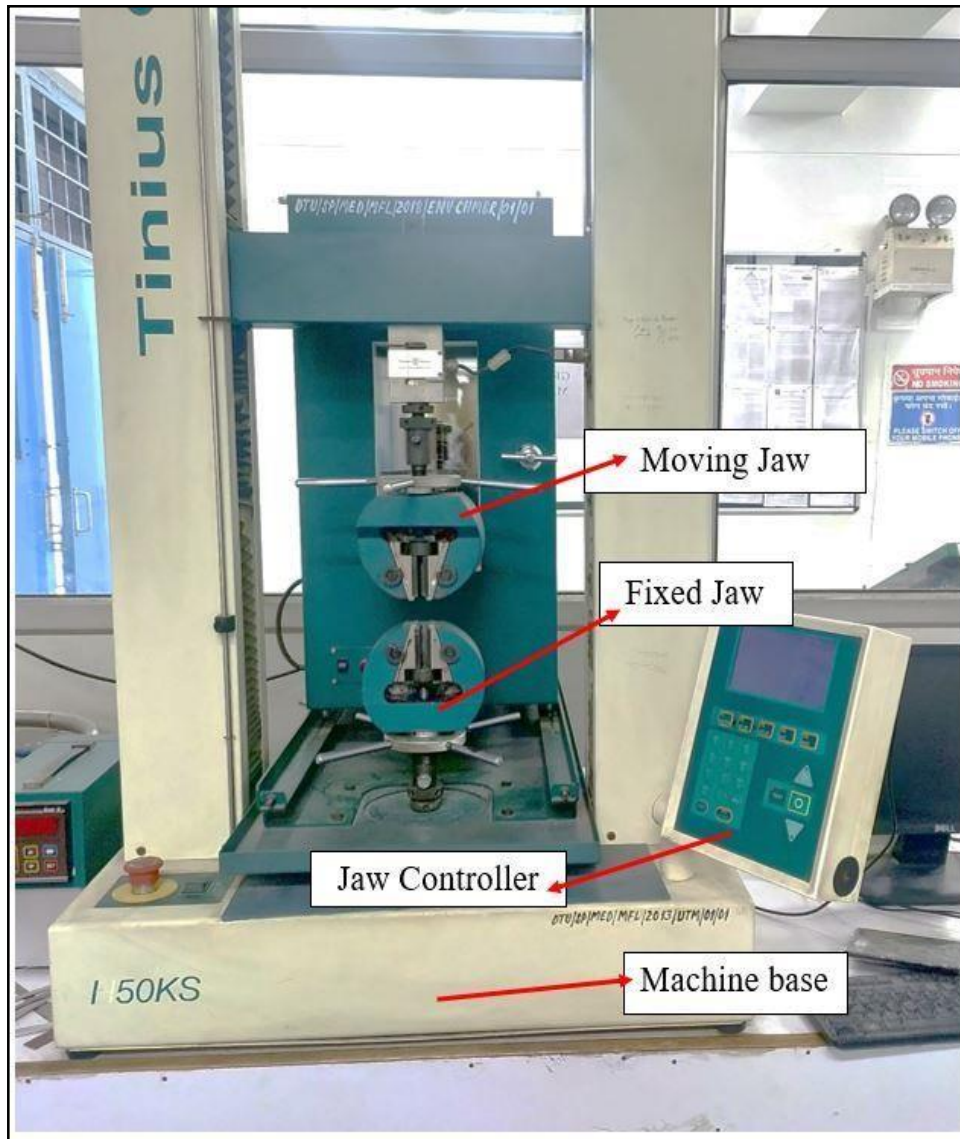


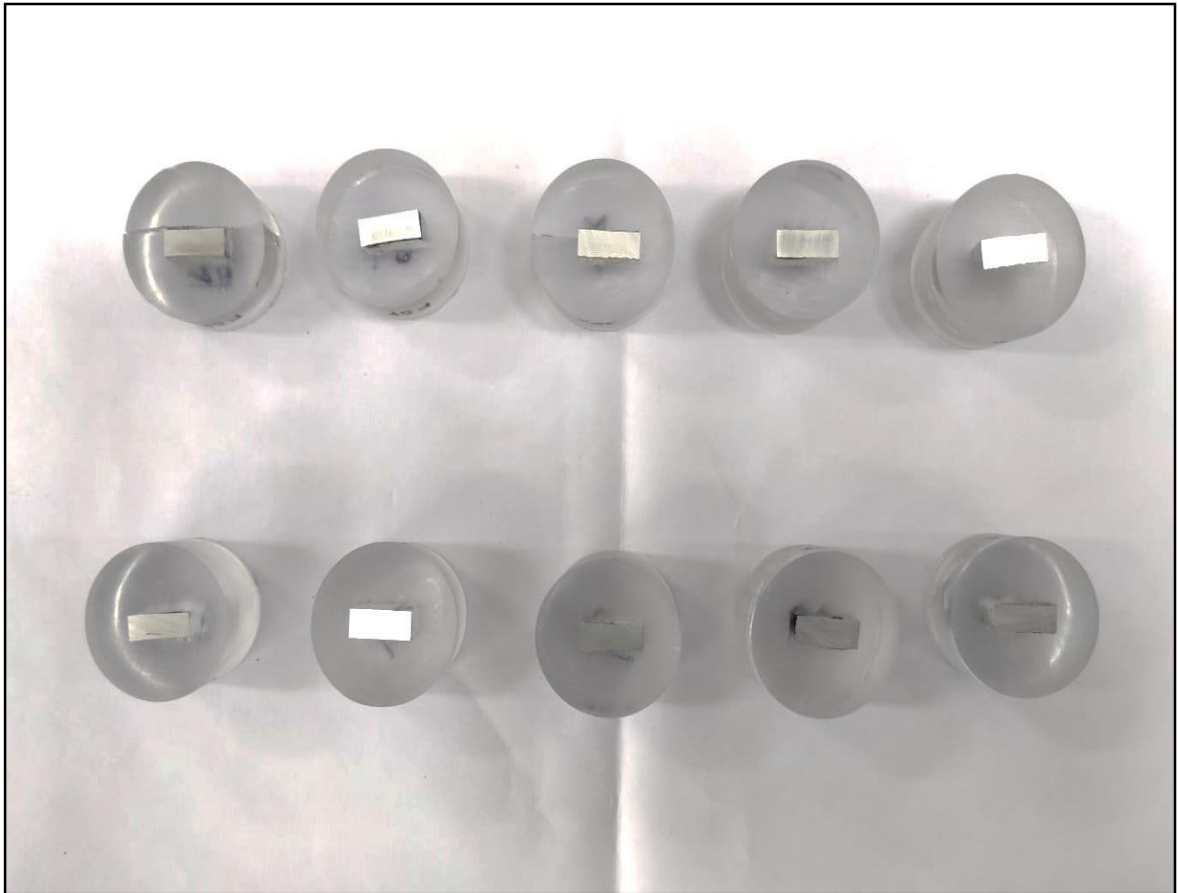
Figure 3.9 UTM Machine, DTU, Delhi

### 3.8 Sample Preparation for micro hardness and microstructure

To conduct the analysis, the targeted region within the material that underwent processing was identified. Subsequently, a wire electro discharge machine was employed to precisely cut specimens with dimensions of 10mm x 10mm x 6mm. To ensure stability during testing,



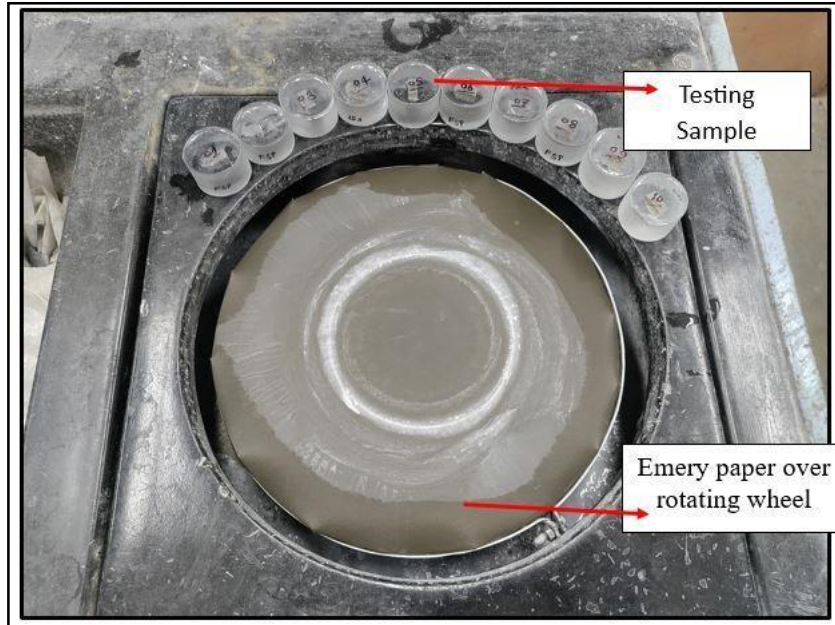
the specimens were securely mounted using epoxy resin in a cold mounting process, preventing any undesired movement or vibration.



*Figure 3.10 samples for microstructure and microhardness test*

### **3.9 Microstructure Testing**

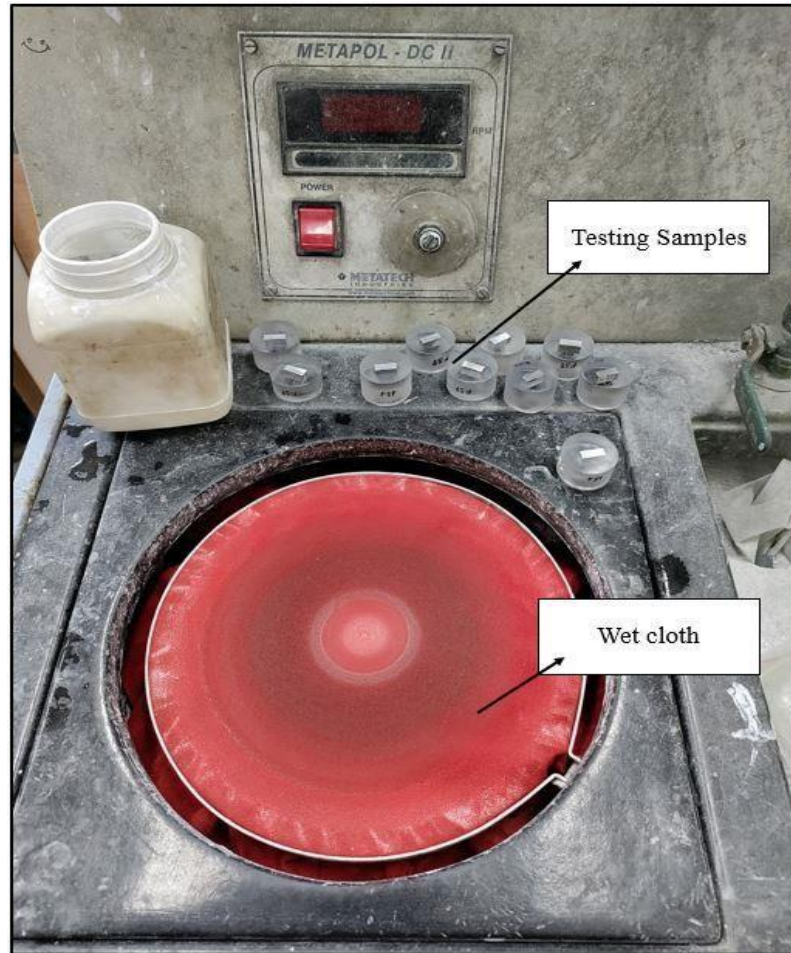
For Microstructure testing dry polishing and wet polishing techniques were utilized. The initial step in the process involved dry polishing, which consisted of utilizing emery paper with varying sizes of the grit. It refers to the coarseness of particles on the paper's surface. Lower grit size means the paper's surface is rough. The progression started with a relatively rough grit size of 220 and gradually moved to finer grit sizes such as 320, 400, 600, and 800.



*Figure 3.11 Dry Polishing*

Following the dry polishing, the specimens underwent wet polishing. Unlike dry polishing, this method involved the water usage. Figure illustrates the step-by-step processes involved in both dry and wet polishing.

After the wet polishing process, the specimens were subjected to etching. Etching involves dipping the surface of the specimens in a combined optimal molar ratio mixture of acids such as HCl & nitric acid was utilized to unveil the microstructure of the specimens.



*Figure 3.12 Wet Polishing*

### **3.10 Micro Hardness Test on DRAMIN-40 STRUERS**

Hardness test was conducted utilizing a DRAMIN-40 STRUERS MICRO/MACRO Hardness Tester. The setup of the machine is depicted in Figure. During the test, a load of 500gf was applied, and the processed regions were subjected to a dwell time of 20 seconds on the processed regions. Testing machine used in this experiment is equipped with an optical microscope that provides a magnification of 10x. A diamond indenter is utilized to create an indentation in the shape of a pyramid. Two measurements, d1 (horizontal distance) and d2 (vertical distance) of the pyramid, are taken to determine the indentation size. Based

on these measurements, the machine calculates and displays the HV value, which represents the Vickers Hardness. The HV value is an indicator of the material's hardness, derived from the size of the indentation.

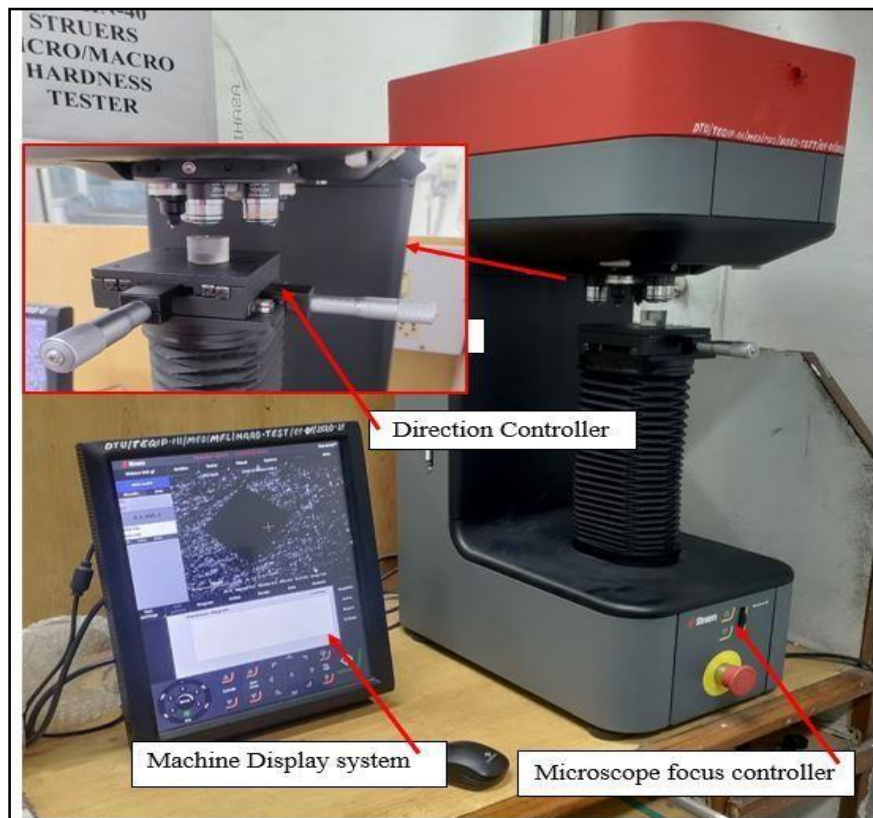


Figure 3.13 DRAMIN-40 Struers Hardness Tester

## **CHAPTER-4**

### **METHODOLOGY**

#### **4.1 Design of Experiment (DOE)**

Design of experiment (DOE) is a structured method for planning, conducting, and analyzing experiments. Its purpose is to gain a deep understanding of how different factors or variables impact the outcome being studied. DOE achieves this by precisely designing and controlling these factors, allowing researchers to observe and measure their effects on the desired response.

#### **4.2 Taguchi Method**

The robust design of experiments, implemented through the Taguchi method, is employed to minimize the variation in a specific process. The primary objective of utilizing this method is to design experiments that can effectively determine the impact of various process parameters on both the mean and variance values of the process performance characteristics. Experimental design of the Taguchi method employs orthogonal arrays to systematically arrange the process parameters. By testing pairs of combinations of these parameters, the Taguchi method enables an efficient exploration of the parameter space. This approach is efficient to identify the factors that have more significant impact and also reduces the number of experiments to be performed.

##### **4.2.1 The steps involved in the implementation of the Taguchi Method are as follows:**

**Define** - The objective is to determine the desired target value for measuring the performance of various process aspects.

**Identify**- The variables within the process have been identified such as tool rotational speed,

tool transverse speed, Hybrid reinforcement. Expanding the no. of levels for a parameter leads to an increase in the number of experiments required

**Create** – An Orthogonal array has to be created that represents the parameter design, No. of experiments.

**Conduct**- The experiments need to be performed as part of the study to collect the data such as Tensile strength, elongation, Yield strength and Hardness value.

**Analyze**- The collected data is analyzed to assess the impact on the performance of different parameters.

#### 4.2.2 Summary of Design

Table 4.1 Design of experiment

	L1	L2	L3
P1 (RPM)	700	1000	1300
P2 (TTS mm/min)	30	45	60
P3* Walnut shell powder (gm)	2 gm	3 gm	4gm

\*Hybrid Reinforcement of SiC (8gm) and Walnut Shell Powder in gm

Table 4.2 L9 Orthogonal Array

Samples	Rotational Speed (RPM)	Tool Transverse speed (mm/min)	Walnut Shell Powder (gm)
1	700	30	2
2	700	45	3
3	700	60	4
4	1000	30	3
5	1000	45	4
6	1000	60	2
7	1300	30	4
8	1300	45	2
9	1300	60	3

### 4.3 Minitab software, Signal to Noise (S/N) ratio

S/N Ratio Analysis is a statistical technique used to evaluate the quality of a process or product.

It helps to identify the optimal combination of input variables that result in the desired output response.

The S/N ratio is a measure of the signal strength (desired output) relative to the noise (undesirable variation).

There are different types of S/N ratios used in different scenarios, such as maximizing response (larger is better), minimizing response (smaller is better), or achieving a target value.

In the context of Signal-to-Noise (S/N) ratios, the coefficients, SE coefficients, T-values, and P-values provide important information about the factors and their impact on the desired output.

**Coefficients:** The coefficients represent the estimated effect of each factor on the S/N ratio. They indicate the magnitude and direction of the influence. Positive coefficients mean that increasing the factor value improves the S/N ratio, while negative coefficients suggest that decreasing the factor value is beneficial.

**SE Coefficients:** SE (Standard Error) coefficients measure the precision of the estimated coefficients. They help determine the reliability of the coefficient estimates. Smaller SE coefficients indicate more reliable estimates, while larger SE coefficients indicate more uncertainty.

**T-values:** T-values are calculated by dividing the coefficient estimate by its corresponding SE coefficient. They indicate the statistical significance of the factor's effect on the S/N ratio. Larger T-values suggest a more significant impact of the factor, while smaller T-values indicate a less significant influence.

**P-values:** P-values are associated with T-values and indicate the probability of observing a T-value as extreme as the one calculated, assuming there is no true effect of the factor. A smaller P-value (typically less than 0.05) suggests that the factor has a significant effect on the S/N ratio.



#### 4.4 Design Expert software for regression equations

It is a powerful tool used for data analysis and experimental design. It includes a feature called "Regression Equations," which helps in developing mathematical models to describe the relationship between input factors (variables) and the response (output) in a regression analysis.

With Design Expert, we can input our experimental data and perform regression analysis to create mathematical equations that represent the relationship between the input factors and the response.

These regression equations allow us to predict the response value based on the given input factor values. They provide insights into the effect of each input factor and their interactions on the response variable. By analyzing the regression equations, we can understand how changes in the input factors impact the response and make informed decisions to optimize your process or system.

#### Final Equations of UTS, Hardness, % Elongation in Terms of Actual Factors:

$$\text{UTS} = (+103.66246 - 0.46906 * \text{TRS} + 3.10752 * \text{TTS} + 199.88158 * \text{WSP} + 9.20797\text{E-}003 * \text{TRS} * \text{TTS} - 0.011107 * \text{TRS} * \text{WSP} - 3.95745 * \text{TTS} * \text{WSP})$$

$$\text{HARDNESS} = (+50.42540 - 0.030940 * \text{TRS} + 0.27162 * \text{TTS} + 15.39571 * \text{WSP} + 6.49206\text{E-}004 * \text{TRS} * \text{TTS} - 1.70952\text{E-}003 * \text{TRS} * \text{WSP} - 0.29038 * \text{TTS} * \text{WSP})$$

$$\text{ELONGATION} = (+3.47302 + 0.013365 * \text{TRS} - 0.56254 * \text{TTS} + 12.00000 * \text{WSP} + 4.76190\text{E-}004 * \text{TRS} * \text{TTS} - 0.010571 * \text{TRS} * \text{WSP} + 0.020952 * \text{TTS} * \text{WSP})$$

## Chapter 5

### Results & Discussions

#### 5.1 Orthogonal array

An orthogonal array is a structured arrangement of experimental factors or variables used in design of experiments (DOE). It is a tabular representation that helps ensure a well-balanced and efficient experiment design. The array is constructed in such a way that each column represents a different factor or variable, and each row represents a specific combination of factor levels.

*Table 4.3 L9 Orthogonal Array*

Samples	Rotational Speed (RPM)	Tool Transverse speed (mm/min)	Walnut Shell Powder (gm)
1	700	30	2
2	700	45	3
3	700	60	4
4	1000	30	3
5	1000	45	4

Samples	Rotational Speed(RPM)	Tool Transverse speed (mm/min)	Walnut Shell Powder (gm)
<b>6</b>	1000	60	2
<b>7</b>	1300	30	4
<b>8</b>	1300	45	2
<b>9</b>	1300	60	3

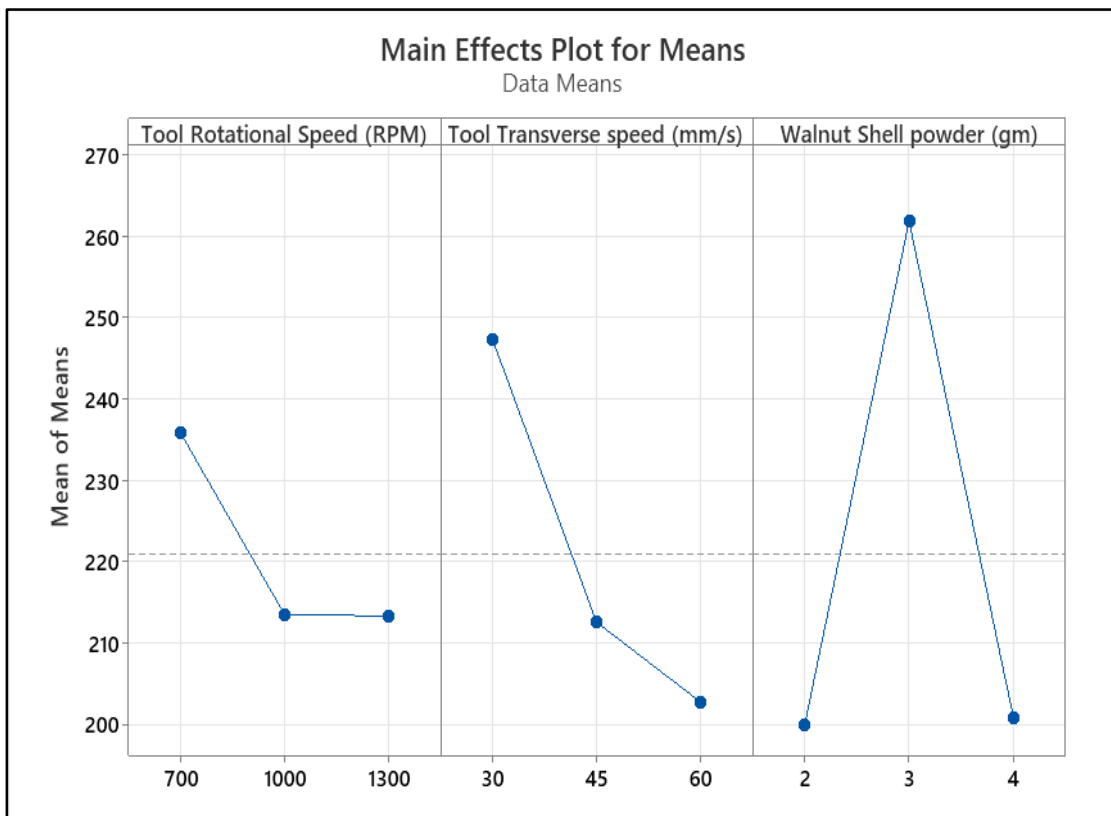
Table 4.4 Observation table

	Rotational Speed (RPM)	Tool Transverse speed (mm/ min)	Walnut shell powder(gm )	UTS (MPa )	Hardness(HV 0.5)	Yield stresses (MPa)	% Elongation
<b>1</b>	700	30	2	198.17	60.9	172.07	16.8
<b>2</b>	700	45	3	254.32	63.72	148.00	19.6
<b>3</b>	700	60	4	175.90	59.77	133.50	14
<b>4</b>	1000	30	3	249.24	61.72	151.39	18.4
<b>5</b>	1000	45	4	189.50	60.9	137.13	24
<b>6</b>	1000	60	2	272.67	65.64	160.57	16.8
<b>7</b>	1300	30	4	214.86	63.73	123.23	18.2
<b>8</b>	1300	45	2	169.60	59.86	141.20	22.8
<b>9</b>	1300	60	3	263.58	65.5	160.69	18

## 5.2 Taguchi Analysis:

Taguchi analysis involves conducting a series of experiments where different factors or variables are varied systematically. These factors can include material properties, process parameters, or design features that may influence the outcome.

### 5.2.1 UTS (MPa) versus Tool Rotational Speed (RPM), Tool Transverse speed (mm/min), Walnut Shell powder (gm)



### 5.2.2 Signal to Noise Ratios table

Larger is better

Level	Tool Rotational Speed (RPM)	Tool Transverse speed (mm/min)	Walnut Shell powder (gm)
1	47.36	47.82	45.87
2	46.41	46.42	48.35
3	46.49	46.02	46.05
`Delta	0.94	1.80	2.49
Rank	3	2	1

### 5.2.3 Response Table for Means

Level	Tool Rotational Speed (RPM)	Tool Transverse speed (mm/min)	WalnutShell powder(gm)
1	235.8	247.3	199.9
2	213.5	212.6	261.8
3	213.3	202.8	200.9
Delta	22.5	44.5	61.9
Rank	3	2	1

#### 5.2.4 Model Coefficients for SN ratios (estimated)

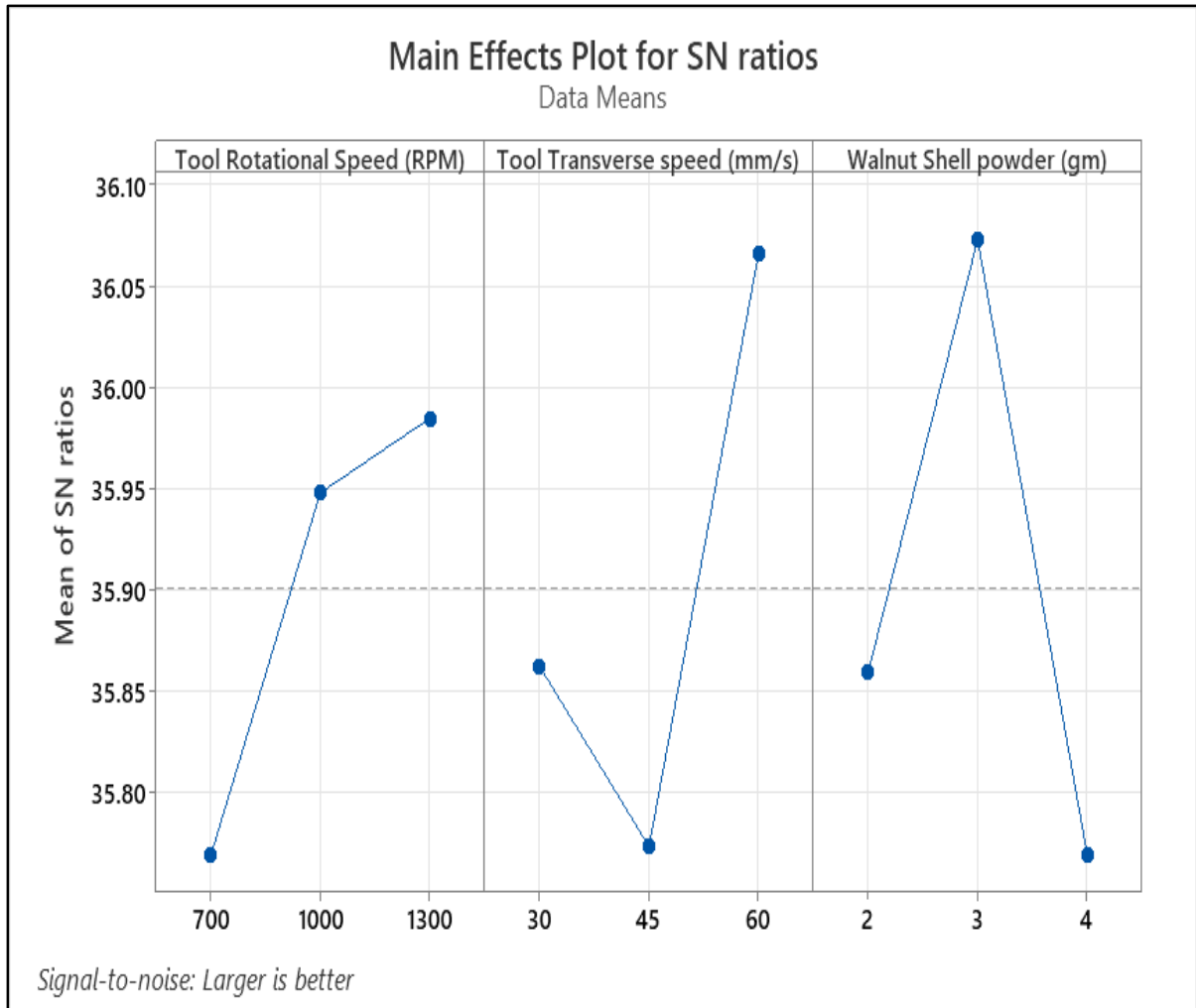
Term	Coef	SE Coef	T	P
Constant	46.7559	0.2891	161.733	0.000
Tool Rot700	0.6034	0.4088	1.476	0.278
Tool Rot1000	-0.3412	0.4088	-0.834	0.492
Tool Tra30	1.0659	0.4088	2.607	0.121
Tool Tra45	-0.3338	0.4088	-0.817	0.500
Walnut S2	-0.8890	0.4088	-2.174	0.162
Walnut S3	1.5986	0.4088	3.910	0.060

**Tool Rotational Speed:** The S/N ratio decreases as the tool rotational speed decreases. Level 1 (235.8 RPM) has the highest S/N ratio, indicating that a higher rotational speed results in a more desirable signal strength relative to noise. Level 2 (213.5 RPM) and Level 3 (213.3 RPM) have lower S/N ratios.

**Tool Transverse Speed:** The S/N ratio is highest at Level 1 (247.3 mm/min), indicating that a higher transverse speed results in a more desirable signal strength relative to noise. Level 3 (202.8 mm/min) has the second-highest S/N ratio, while Level 2 (212.6 mm/min) has the lowest S/N ratio.

**Walnut Shell Powder:** The S/N ratio is highest at Level 1 (199.9 gm), indicating that a lower amount of walnut shell powder results in a more desirable signal strength relative to noise. Level 3 (200.9 gm) has the second-highest S/N ratio, while Level 2 (261.8 gm) has the lowest S/N ratio.

**5.3 Hardness HV0.5 versus Tool Rotational Speed (RPM), Tool Transverse speed (mm/min), Walnut Shell powder (gm)**



### 5.3.1 Signal to Noise Ratios table

Larger is better

<b>Level</b>	<b>Tool Rotational Speed (RPM)</b>	<b>Tool Transverse speed (mm/min)</b>	<b>Walnut Shell powder (gm)</b>
<b>1</b>	35.77	35.86	35.86
<b>2</b>	35.95	35.77	36.07
<b>3</b>	35.98	36.07	35.77
<b>Delta</b>	0.22	0.29	0.30
<b>Rank</b>	3	2	1

### 5.3.2 Response Table for Means

<b>Level</b>	<b>Tool Rotational Speed (RPM)</b>	<b>Tool Transverse speed (mm/min)</b>	<b>Walnut Shell powder (gm)</b>
1	61.46	62.12	62.13
2	62.75	61.49	63.65



<b>Level</b>	<b>Tool Rotational Speed (RPM)</b>	<b>Tool Transverse speed (mm/min)</b>	<b>Walnut Shell powder (gm)</b>
3	63.03	63.64	61.47
Delta	1.57	2.14	2.18
Rank	3	2	1

<b>Term</b>	<b>Coef</b>	<b>SE Coef</b>	<b>T</b>	<b>P</b>
Constant	35.9007	0.1573	228.204	0.000
Tool Rot 700	-0.1315	0.2225	-0.591	0.614
Tool Rot 1000	0.0474	0.2225	0.213	0.851
Tool Tra 30	-0.0381	0.2225	-0.171	0.880
Tool Tra 45	-0.1272	0.2225	-0.572	0.625
Walnut S 2	-0.0412	0.2225	-0.185	0.870
Walnut S 3	0.1723	0.2225	0.774	0.520

### 5.3.3 Model Coefficients for SN ratios (estimated)

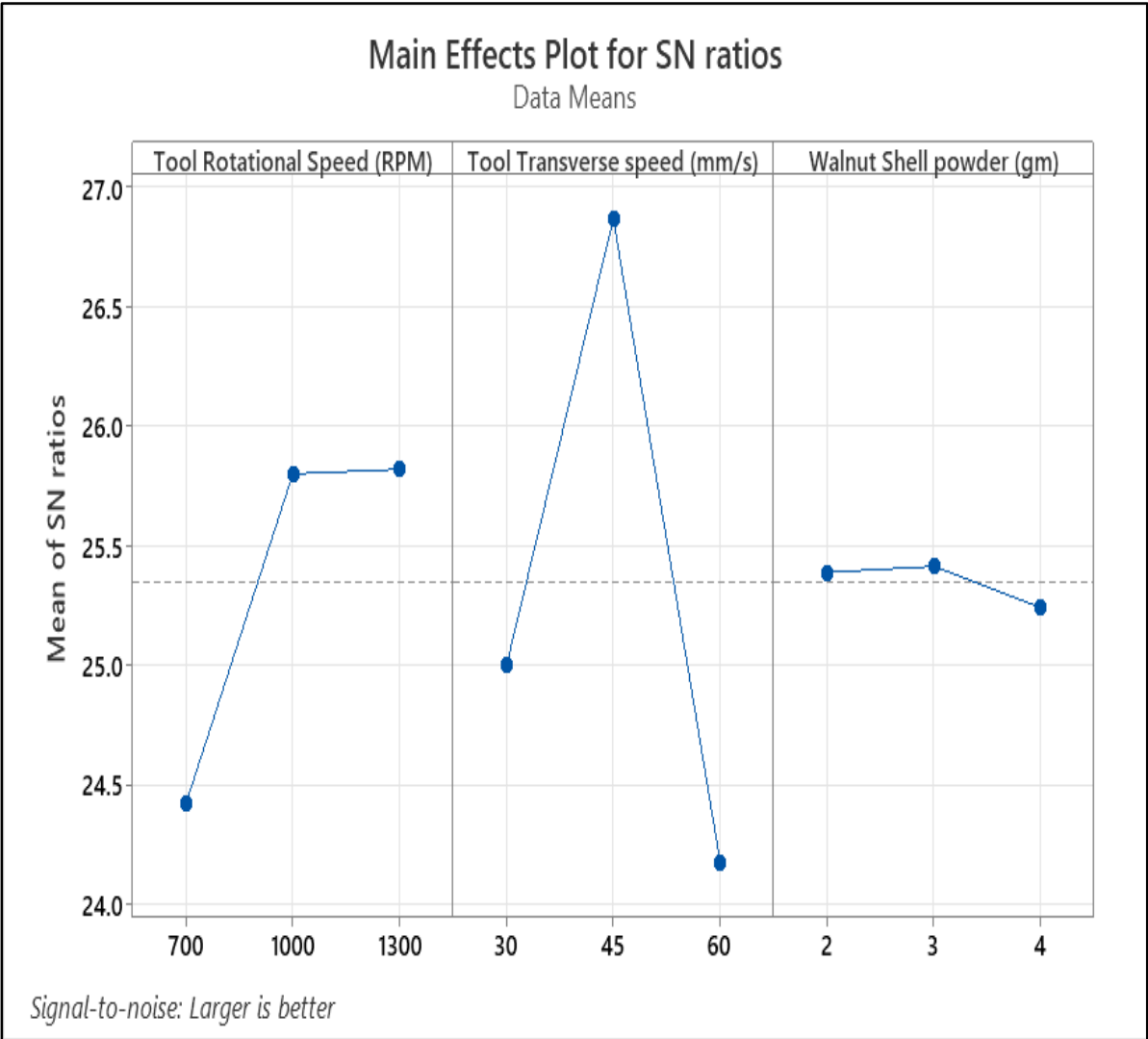
**Tool Rotational Speed:** The means of the response variables (Tool Rotational Speed) at each level are relatively close to each other. The S/N ratios show minimal differences between the levels, with Level 3 (63.03 RPM) having the highest mean value, followed closely by Level 2 (62.75 RPM) and Level 1 (61.46 RPM). Therefore, the tool rotational speed does not have a significant impact on the response variable.

**Tool Transverse Speed:** The means of the response variables (Tool Transverse Speed) also exhibit minimal differences between the levels. Level 3 (63.64 mm/min) has the highest mean value, followed by Level 1 (62.12 mm/min) and Level 2 (61.49 mm/min). Similar to the tool rotational speed, the tool transverse speed does not show a clear pattern of impact on the response variable.

**Walnut Shell Powder:** The means of the response variables (Walnut Shell Powder) show slightly more variation between the levels. Level 1 has (62.13 gm) mean value, Level 2 has highest mean value of (63.65 gm) and level 3 has 61.47.

**Delta:** The Delta values represent the differences in means between different levels. In this case, the Delta values for all three factors (Tool Rotational Speed, Tool Transverse Speed, and Walnut Shell Powder) are relatively small, indicating that the factors do not have a significant impact on the response variable.

**5.4 % Elongation versus Tool Rotational Speed (RPM), Tool Transverse speed (mm/min), Walnut Shell powder (gm)**



#### 5.4.1 Signal to Noise Ratios table

Larger is better

<b>Level</b>	<b>Tool Rotational Speed (RPM)</b>	<b>Tool Transverse speed (mm/min)</b>	<b>Walnut Shell powder (gm)</b>
1	24.42	25.00	25.39
2	25.80	26.87	25.42
3	25.82	24.18	25.24
Delta	1.40	2.69	0.17
Rank	2	1	3

#### 5.4.2 Response Table for Means

<b>Level</b>	<b>Tool Rotational Speed (RPM)</b>	<b>Tool Transverse speed (mm/min)</b>	<b>Walnut Shell powder (gm)</b>
1	16.80	17.80	18.80
2	19.73	22.13	18.67
3	19.67	16.27	18.73
Delta	2.93	5.87	0.13
Rank	2	1	3

#### 5.4.3 Model Coefficients for SN ratios (estimated)

Term	Coef	SE Coef	T	P
Constant	25.3496	0.1952	129.832	0.000
Tool Rot 700	-0.9250	0.2761	-3.350	0.079
Tool Rot 1000	0.4527	0.2761	1.639	0.243
Tool Tra 30	-0.3483	0.2761	-1.261	0.334
Tool Tra 45	1.5198	0.2761	5.504	0.031
Walnut S 2	0.0408	0.2761	0.148	0.896
Walnut S 3	0.0661	0.2761	0.239	0.833

**Tool Rotational Speed:** The S/N ratio increases as the tool rotational speed increases. Level 3 (19.67 RPM) has the highest S/N ratio, indicating that a higher rotational speed results in a more desirable signal strength relative to noise. Level 2 (19.73 RPM) and Level 1 (16.80 RPM) have lower S/N ratios.

**Tool Transverse Speed:** The S/N ratio is highest at Level 2 (22.13 mm/min), Level 3 (16.27 mm/min), while Level 1 (17.80 mm/min) has the second-highest S/N ratio the lowest S/N ratio.

**Walnut Shell Powder:** The S/N ratio remains relatively consistent across different levels of walnut shell powder. Level 2 (18.67 gm) has the highest S/N ratio, followed closely by Level 3 (18.73 gm) and Level 1 (18.80 gm). The differences in S/N ratio between these

levels are minimal.

**Delta:** The Delta values represent the differences in S/N ratios between different levels. A larger Delta indicates a greater impact on the S/N ratio. In this case, the tool transverse speed has the highest Delta value (5.87), followed by the tool rotational speed (2.93), and the walnut shell powder (0.13).

### 5.5 Results for Tensile test



*Figure 5.1 Tensile specimens*

On conducting tensile tests on all ASTM E8 tensile standard samples, it can be concluded that the tensile test was not compromised at the centerline where the groove was created and filled with reinforcement prior to processing. This observation indicates that the strength of the plate increased on using SiC and Walnut Shell Powder as reinforcements.

During the test, crucial parameters such as Tensile strength, % elongation and Yield strength were measured & recorded. These measurements offer valuable insights into the material's mechanical properties and its capacity to endure stretching or elongation before failure.

The highest Ultimate Tensile Strength (UTS) observed is 272.7 MPa, which corresponds to a Tool Rotational Speed of 1000 RPM, Tool Transverse speed of 30 mm/min, and Walnut Shell powder of 3 gm.

### 5.6 Results for Hardness test

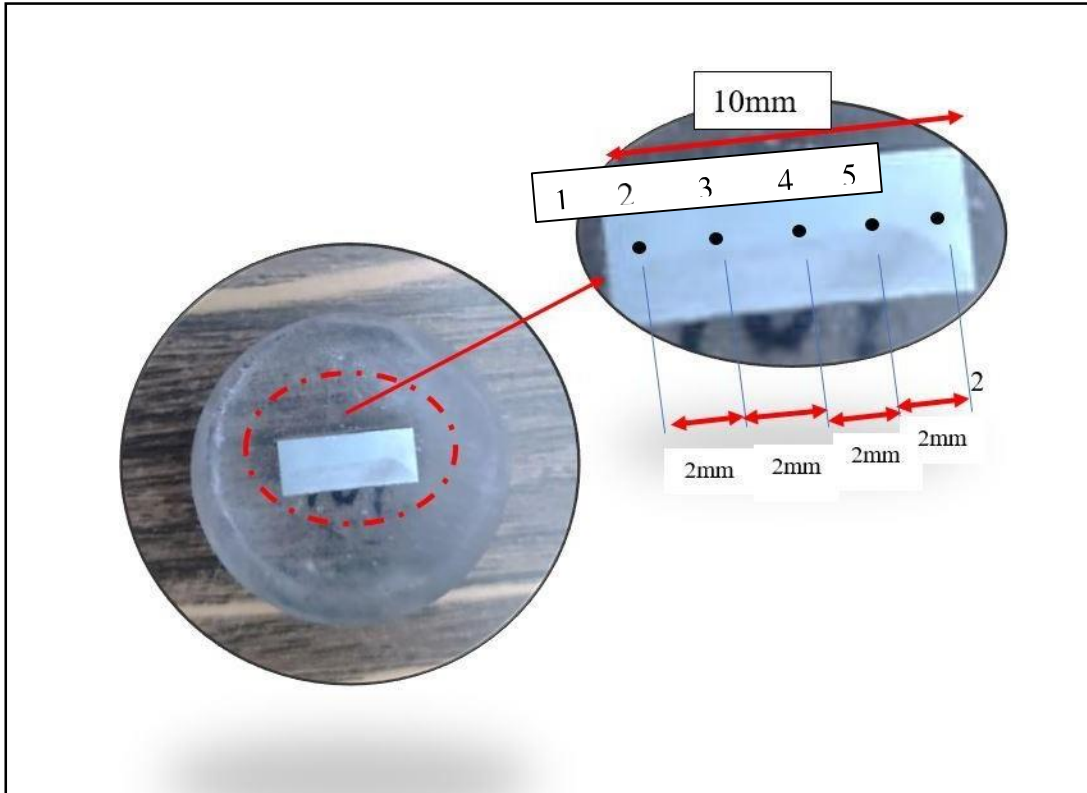
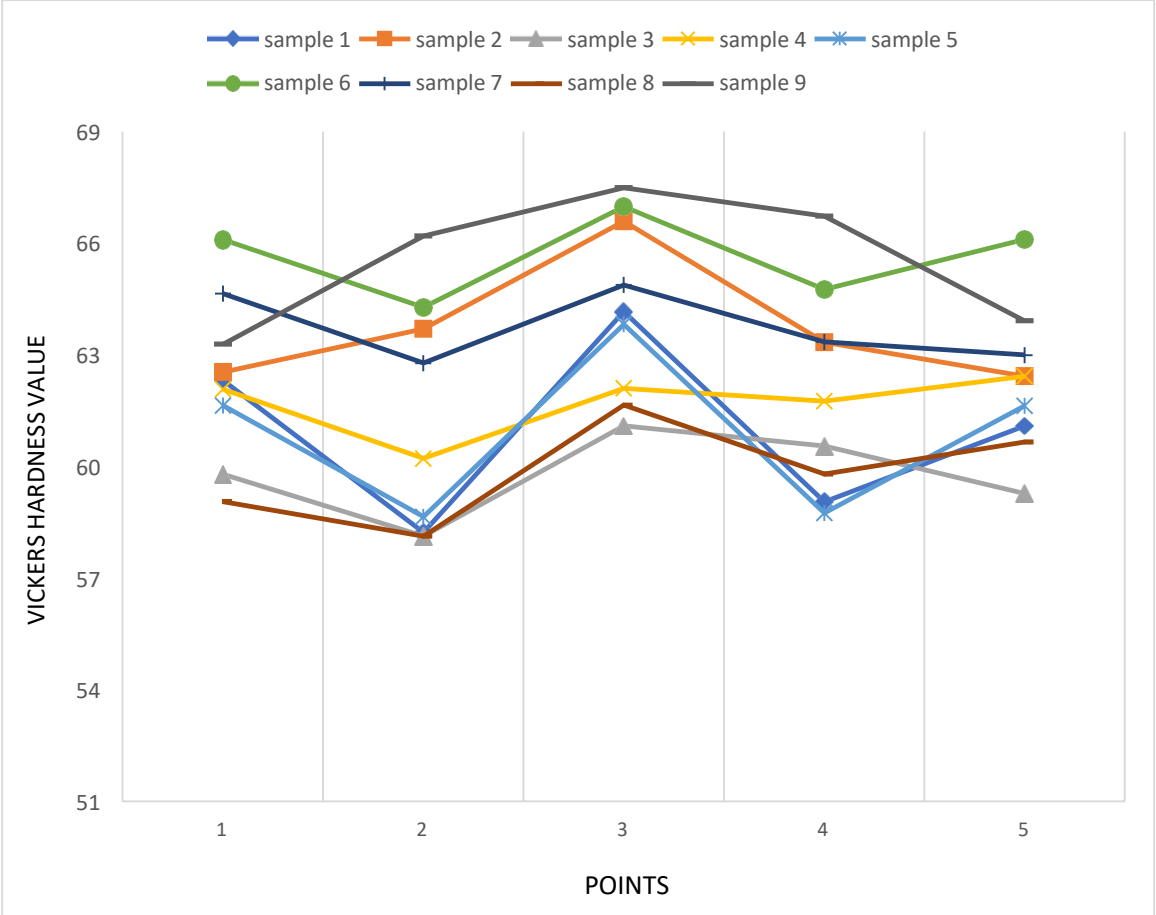


Figure 5.2 Hardness test specimen

To conduct the micro hardness test, specimens of 10mm\*10mm piece was cut from the Friction Stir Processed area using a wire electro discharge machine. The cut specimen was then carefully mounted using epoxy resin in a cold mounting process. Afterward, the specimen underwent dry and wet polishing. For the hardness test, five points on the specimen were considered, each spaced 2mm apart, and the hardness was measured at these points as shown in the fig. 5.3

The highest hardness value observed is 65.64 (HV 0.5), which corresponds to a Tool Rotational Speed of 1000 RPM, Tool Transverse speed of 60 mm/min, and Walnut Shell powder of 2 gm.

Figure 5.3 Vickers Hardness graph

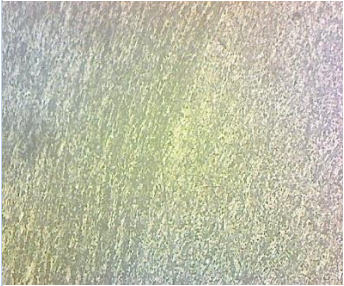

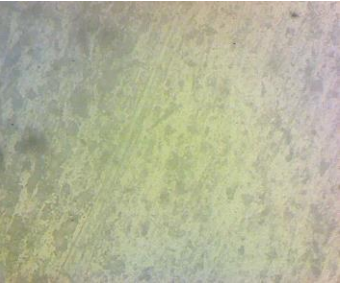
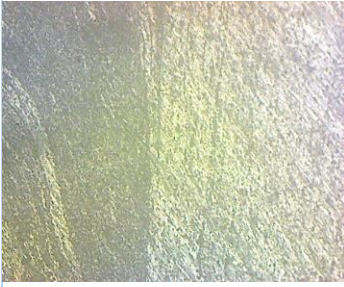
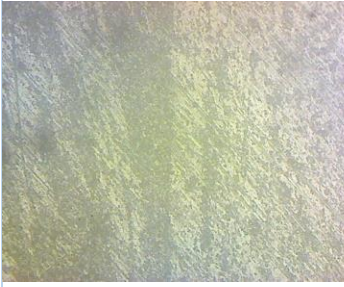
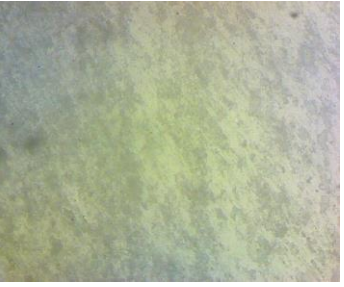


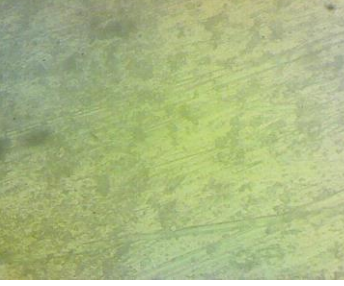


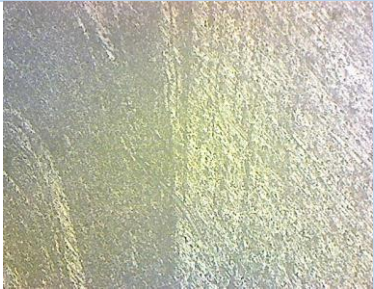
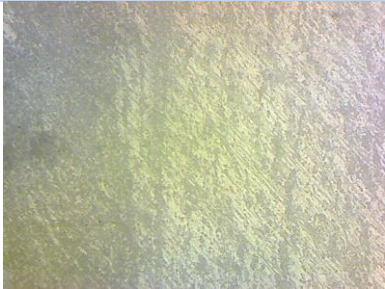



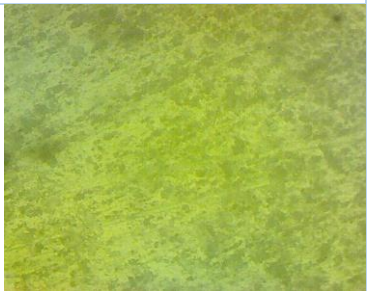







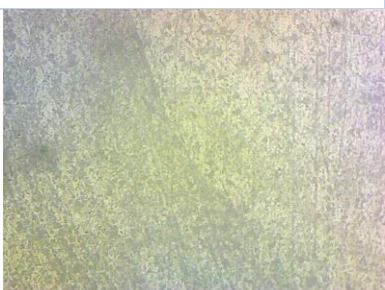

Sample 6 consistently shows the highest mean hardness values among all the samples. which corresponds to a Tool Rotational Speed of 1000 RPM, Tool Transverse speed of 60 mm/min, and Walnut Shell powder of 2 gm. And samples 3, 7, and 9 also exhibit relatively high hardness values, indicating good hardness properties.

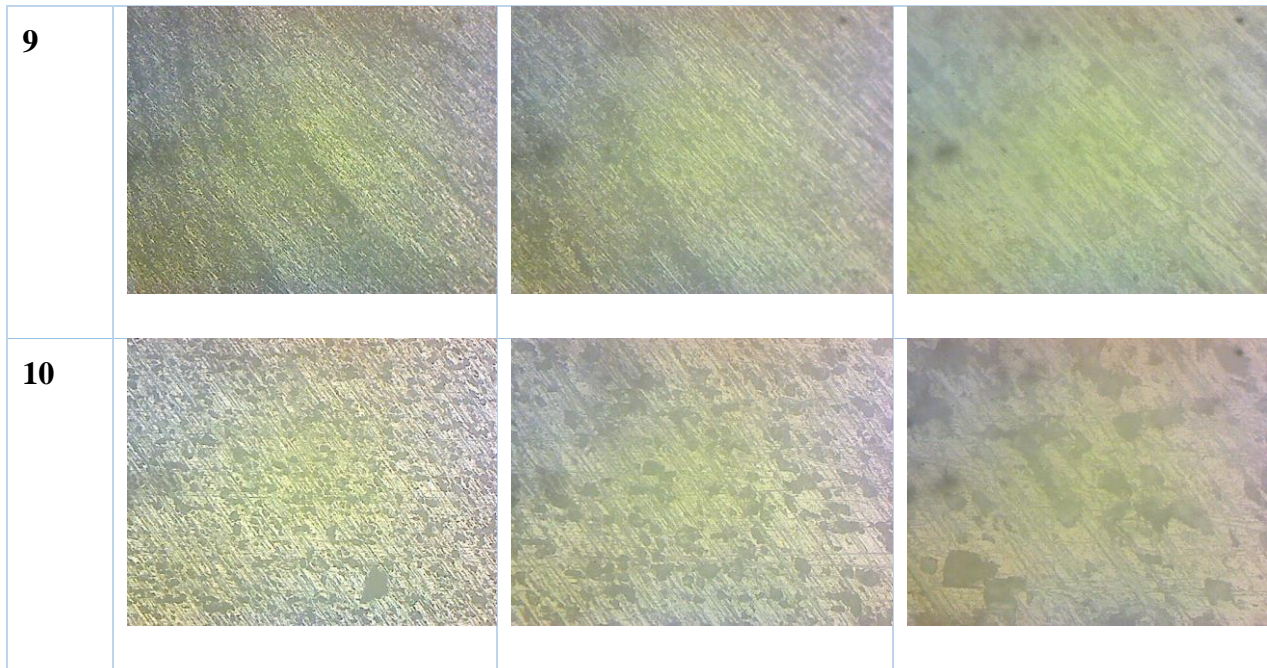


## 5.7 Results for Microstructure test

Figure 5.4 optical microscopy images at 100x, 200x and 500x

S.N.	100X	200X	500X
1			
2			
3			
4			

			
<b>5</b>			
<b>6</b>			
<b>7</b>			
<b>8</b>			



### 5.8 Microstructure Analysis

Microstructure analysis was carried out using an optical microscope available in the university metallurgy lab. And the following conclusions that can be drawn are as under:

1. **Increase strength:** On performing FSP grain refinement can be seen. Grain refinement increases the strength of the material by hindering the dislocation. Smaller grains have more grain boundaries which also act as barrier to the dislocation movement hence resulting in high hardness & material strength.
2. **Mechanical properties:** It has also improved the mechanical properties of aluminium such as tensile strength, Fatigue resistance. It increases the materials ability to withstand the applied loads.
3. **Increased Toughness:** Grain refinement in aluminium increase its toughness, which means the ability to absorb energy before fracture. Smaller grains can distribute stress more uniformly, prevent the chances of concentration of stress.

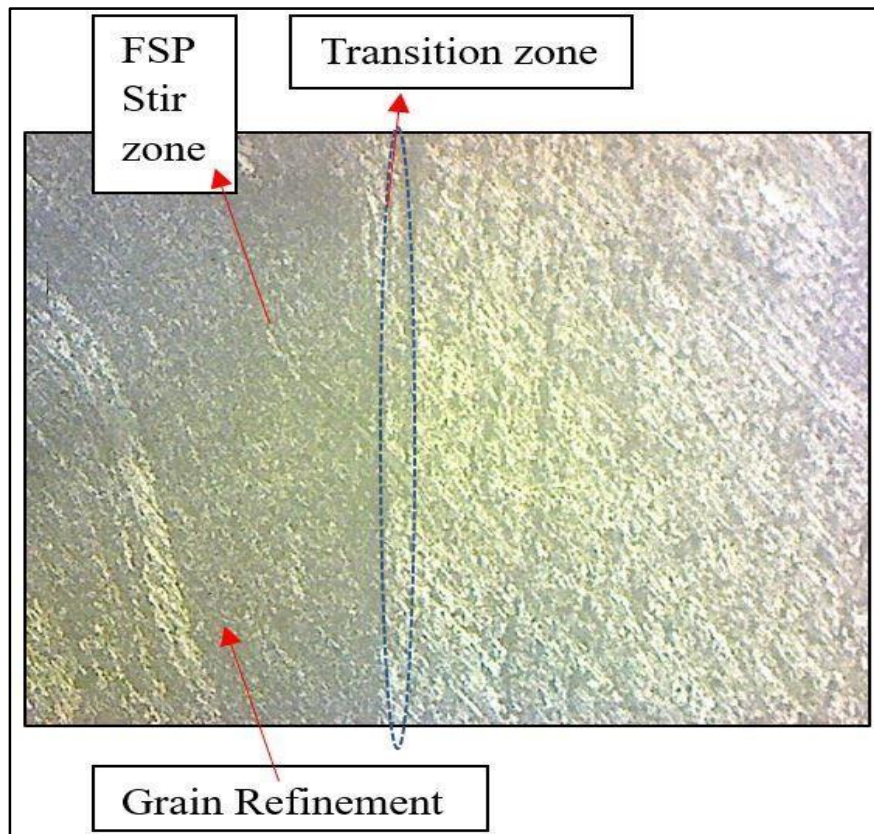


Figure 5.5 Microstructure analysis

Friction Stir Zone (FSZ): refers to the area in the material that has been directly affected by the rotating tool during the FSP process. It is the region where the material experiences intense heat and mechanical deformation. The rotating tool generates friction and applies pressure to the material, causing it to soften and undergo plastic deformation. As a result, the material in the friction stir zone undergoes significant microstructural changes, such as grain refinement and the formation of a distinctive stirred pattern.

Transition Zone: The transition zone, also known as the heat-affected zone (HAZ), is the region adjacent to the friction stir zone. It is characterized by a gradual transition in microstructure and properties between the affected materials in the friction stir zone and the unaffected base material. The transition zone experiences some heat input from the friction stir process but doesn't undergo the same level of deformation as the friction stir zone.

## CHAPTER 6

### CONCLUSION AND FUTURE SCOPE OF STUDY

#### 6.1 Conclusions

The following conclusions can be drawn regarding the friction stir processing (FSP) of AA6082 using silicon carbide (SiC) reinforcement and walnut shell powder:

- The highest Ultimate Tensile Strength (UTS) observed is 272.7 MPa, which corresponds to a Tool Rotational Speed of 1000 RPM, Tool Transverse speed of 30 mm/min, and Walnut Shell powder of 3 gm.
- The base metal had a tensile strength of 237.72 MPa. Therefore, the tensile strength has increased by approximately 14.7% after performing the FSP process with reinforcement.
- The maximum elongation observed was 24.0% for a tool rotational speed of 1000 RPM, tool transverse speed of 45 mm/min, and walnut shell powder content of 4 gm. It varied with different combinations of process parameters, indicating the influence of tool rotational speed, tool transverse speed, and walnut shell powder content on the ductility of the material.
- The highest hardness value observed is 65.64 (HV 0.5), which corresponds to a Tool Rotational Speed of 1000 RPM, Tool Transverse speed of 60 mm/min, and Walnut Shell powder of 2 gm.
- The base metal had a hardness value of 58 (HV 0.5) Therefore, the hardness has increased by approximately 13.17% after performing the FSP process with reinforcement.

## 6.2 Future scope of the study

The future possibilities of using Friction Stir Processing (FSP) on AA6082 hold great potential for further advancements.

**Different Reinforcements:** Investigating the effects of various reinforcements, such as ceramic particles, metallic additives, or hybrid reinforcements, can provide valuable insights into their influence on the mechanical properties, microstructure, and performance of the processed material.

**Variation in Tool Profiles:** Studying the impact of different tool shapes, such as cylindrical, threaded, or tapered, and tool profiles, including smooth or modified profiles, can offer new possibilities for controlling the material flow, heat distribution, and resulting microstructure during FSP. This research can lead to the development of optimized tool designs for enhanced process efficiency and improved material properties.

**Analysis of Residual Stress:** Investigating the residual stress distribution in FSP-treated AA6082 samples can provide valuable information about the structural integrity and stability of the processed material

**XRD Analysis:** Employing X-ray Diffraction (XRD) analysis can enable the identification and characterization of phases present in the FSP-processed AA6082 material

## **CHAPTER 7 REFERENCES**

1. M.M. El-Rayes, E.A. El-Danaf, “The influence of multi-pass friction stir processing on the microstructural and mechanical properties of Aluminum Alloy 6082”, *Journal of Materials Processing Technology* 212 (2012) 1157–1168
2. P L Threadgill, A J Leonard, H R Shercliff and P J Withers “ Friction stir welding of aluminium alloys”, *International Materials Reviews*, vol.54. pp. 49-93.
3. M. Sivanesh Prabhu et al., “Friction and wear measurements of friction stir processed aluminium alloy 6082/CaCO<sub>3</sub> composite”, *Measurement* 142 (2019) 10–20,
4. Hardik Vyas, Kush P. Mehta, “Effect of Multi Pass Friction Stir Processing on Surface Modification and Properties of Aluminum Alloy 6061” *Key Engineering Materials*, Vol. 813, pp 404-410,
5. Shamsipur et al, “Surface Modification of Titanium by Producing Ti/TiN Surface Composite Layers via FSP”, *Acta Metall. Sin. (Engl. Lett.)*, 2017, 30(6), 550–557
6. Balram Yelamasetti, P Naveen Kumar, Venkat Ramana , Kuldeep K Saxena , Velaphi Msomi , Vishwanatha H M4 and Ajit Behera (2023) “Surface modification of aluminum alloy 6061 by embedding B<sub>4</sub>C particles via friction stir processing”, *Mater. Res.Express* 9 (2022) 056511
7. Omar S. Saliha, Hengan Oua, , Xingguo Weib , W. Sun “Microstructure and mechanical properties of friction stir welded AA6092/ SiC metal matrix composite”, *Materials Science and Engineering: A Volume* 742, 10 January 2019, Pages 78-88
8. Peng Li , Yiqi Tong , Xingxing Wang , Yutaka S. Sato , Honggang Dong a, “Microstructures and mechanical properties of AlCoCrFeNi<sub>2.1</sub>/6061-T6 aluminum-matrix composites prepared by friction stir processing”, *Material science & Engineering A* 863 (2023) 144544

9. Yuvaraj, N., & Aravindan, S. (2017). "Comparison studies on mechanical and wear behavior of fabricated aluminum surface nano composites by fusion and solid state processing". *Surface and Coatings Technology*, 309, 309-319
10. Sharifitabar, M., Sarani, A., Khorshahian, S., & Afarani, M. S. (2011). "Fabrication of 5052Al/Al<sub>2</sub>O<sub>3</sub> nanoceramic particle reinforced composite via friction stir processing route". *Materials & Design*, 32(8-9), 4164-4172.
11. Moslem Paidara, Olatunji Oladimeji Ojob , Hamid Reza Ezatpour , Akbar Heidarzadehc "Influence of multi-pass FSP on the microstructure, mechanical properties and tribological characterization of Al/B<sub>4</sub>C composite fabricated by accumulative roll bonding (ARB)" *Surface coatings technology* 361 (2019) 159-169
12. P K Mandal "Surface modification of Aluminium alloy (7xxx series) by multipass friction stir processing", *Global Journal of Engineering and Technology Advances*, 2021, 06(02), 008–017
13. Essam B. Moustafa , Ahmed O. Mosleh "Effect of (TiB) modifier elements and FSP on 5052 aluminum alloy", *Journal of Alloys and Compounds* 823 (2020) 153745
14. Seyed Sajad Mirjavadi , Mohammad Alipour , A.M.S. Hamouda a , Abdolhamid Matin , S. Kord, Behzad Mohasel Afshari , Praveennath G. Koppad "Effect of multi-pass friction stir processing on the microstructure, mechanical and wear properties of AA5083/ZrO<sub>2</sub> nanocomposites", *Journal of Alloys and Compounds* 726 (2017) 1262-1273
15. Sumit Choudhary, Vidit Gaur "Enhanced fatigue properties of AA5086 friction stir weld joints by Cu-reinforcement", *Materials Science & Engineering A* 869 (2023) 144778
16. Essam B. Moustafa, Anastasia V. Mikhaylovskaya, Mohammed A. Taha, Ahmed O. Mosleh "Improvement of the microstructure and mechanical properties by hybridizing the surface of AA7075 by hexagonal boron nitride with carbide particles using the FSP process", *journal of materials research and technology* 2022; 17:1986 – 1999



17. M. Saravana Kumar, M. Vasumathi, S. Rashia Begum b , Scutaru Maria Luminita , Sorin Vlase , Catalin I. Pruncu, “Influence of B4C and industrial waste fly ash reinforcement particles on the micro structural characteristics and mechanical behavior of aluminium (AlMgSi-T6) hybrid metal matrix composite” journal of materials research and technology 2021;15:1201 – 1216
18. Safiye Ipek Ayvaz, Dilek Arslan, Mehmet Ayvaz , “Investigation of mechanical and tribological behavior of SiC and B4C reinforced Al-Zn-Mg-Si-Cu alloy matrix surface composites fabricated via friction stir processing”, Materials Today Communications 31 (2022) 103419
19. Mohd Rashid, N. Yuvraj, Shailesh Kumar Singh “Micro Structural and Mechanical Behaviours of Nano-TiC-Reinforced AA6082” Fusion of Science & Technology, 18-22, 2016
20. B. Praveen KUMAR, Anil Kumar BIRRU “Microstructure and mechanical properties of aluminium metal matrix composites with addition of bamboo leaf ash by stir casting method” Trans. Nonferrous Met. Soc. China 27(2017) 2555–2572
21. Rajeev Kumar, Jujhar Singh , Shubham Sharma, Changhe Li f , Grzegorz Krolczyk, Szymon Wojciechowski, “Neutrosophic entropy-based ingenious measurement for fast fourier transforms based classification of process-parameters and wear resistance of friction-stir processed hybrid AA7075- B4C aluminium metal-matrix composites” journal of materials research and technology 2022;20:720 – 739
22. Nitesh Kumar, Rakesh Kumar Singh, Ashish Kumar Srivastava , Akash Nag, Jana Petru and Sergej Hloch “Surface Modification and Parametric Optimization of Tensile Strength of Al6082/SiC/Waste Material Surface Composite Produced by Friction Stir Processing” Coatings 2022, 12, 1909.
23. Alaneme, K. K, Bodunrin, M. O., & Awe, A. A. (2018). “Microstructure, mechanical and fracture properties of groundnut shell ash and silicon carbide dispersion strengthened aluminium matrix composites.” Journal of King Saud University-Engineering Sciences, 30(1),

96-103.

24. N. Li , L.H. Wu , Z.K. Li , H.M. Fu , Z.W. Zhu , P. Xue , F.C. Liu , D.R. Ni, B.L. Xiao, Z.Y. Ma a, “achieving superior super plasticity in CoCrFeNiCu high entropy alloy via friction stir processing with an improved convex tool” *Materials Science & Engineering A* 873 (2023) 145034
25. T M Harish, Suni Mathai, Manoj George, M Harisankar, Anand G illimattathil, Blitz Francis, Anandu Venugopal, “Development of aluminium 5083/B4C/carbonized coconut shell ash hybrid composite using friction stir processing”, *Materials Today: Proceedings* 72 (2023) 3149–3153
26. Gaurav Rajan , Atul kumar , Ashwin Kumar Godasu , Suhrit Mula, “Effect of friction stir processing on microstructural evolution and mechanical properties of nanosized SiC reinforced AA5083 nanocomposites developed by stir casting” *Materials Today Communications* 35 (2023) 105912
27. Xiguo Chen , Amin Kolooshani b , Behzad Heidarshenas c,\* , Bardia Morteza gholi d , Yanjie Yuan, D.T. Semiruomi, “Effects of tricalcium phosphate-titanium nanoparticles on mechanical performance after friction stir processing on titanium alloys for dental applications” *Materials Science and Engineering B* 293 (2023) 116492
28. Yuchen Peng, Biao Huang, Yuefang Zhong , Changchao Su, Zushan Tao, Xincheng Rong, Zhuoyuan Li, Hongqun Tang a, “Electrochemical corrosion behavior of 6061 Al alloy under high rotating speed submerged friction stir processing”, *Corrosion Science* 215 (2023) 111029
29. Ibrahim H. Zainelabdeen , Fadi A. Al-Badour, Akeem Yusuf Adesina , Rami Suleiman, Fadi A. Ghaith “Friction stir surface processing of 6061 aluminum alloy for superior corrosion resistance and enhanced microhardness”, *International Journal of Lightweight Materials and Manufacture* 6 (2023) 129-139
30. Changshu Hea, Jingxun Wei , Ying Li, Zhiqiang Zhanga,b , Ni Tiana,b,c , Gaowu Qina,b,c , Liang Zuoa “Improvement of microstructure and fatigue performance of wire-arc additive manufactured 4043 aluminum alloy assisted by interlayer friction stir processing”, *Journal of Materials Science & Technology* 133 (2023) 183–194

31. Suhong Zhang, Yuan Li, Alan Frederick , Yanli Wang , Yiyu Wang , Lawrence Allard Jr. b , Michael Koehler , Seungha Shin , Anming Hu , Zhili Feng , “In-situ formation of Al<sub>3</sub>Ni nano particles in synthesis of Al 7075 alloy by friction stir processing with Ni powder addition”, *Journal of Materials Processing Tech.* 311 (2023) 117803
32. S. Ragu Nathan, K. Suganeswaran, Surya Kumar, P. Thangavel, V.K. Gobinath b “Investigations on microstructure, thermo-mechanical and tribological behavior of graphene oxide reinforced AA7075 surface composites developed via friction stir processing”, *Journal of Manufacturing Processes* 90 (2023) 139–150
33. A.K. Basak, A. Pramanik, C. Prakash , S. Shankar, Satbir S. Sehgal “Microstructure and micro-mechanical properties of friction stir processed Al 5086-based surface composite”, *Materials Today Communications* 35 (2023) 105830
34. Wenchang Li, Xuesong Li, Yunfeng Li “Microstructure and properties of carbon fiber-H62 brass matrix composites prepared by friction stir processing”, *Journal of King Saud University – Science* 35 (2023) 102652
35. Krunal M. Mehta, Vishvesh J. Badheka “Wear behavior of Al-6061-B<sub>4</sub>C surface composites fabricated by Friction Stir Processing using Slot and Hole method of reinforcement” application *Wear* 522 (2023) 204719